Design of Total Runoff Integrating Pathways (TRIP)—A Global River Channel Network

Taikan Oki* and Y. C. Sud**

NASA/Goddard Space Flight Center, Greenbelt, Maryland

ABSTRACT: As a first step toward designing a comprehensive model for validating land surface hydrology and river flow in Earth system models, a global river channel network has been prepared at 1° latitude × 1° longitude resolution. The end product is the Total Runoff Integrating Pathways (TRIP) network. The aim of TRIP is to provide information of lateral water movement over land following the paths of river channels. Flow directions were determined from vector data of river channels and river pathways available in two recent atlases; however, an automatic procedure using a digital elevation map of the corresponding horizontal resolution was used as a first guess. In this way, a template to convert the river discharge data into mean runoff per unit area of the basin has been obtained. One hundred eighty major rivers are identified and adequately resolved; they cover 63% of land, excluding Antarctica and Greenland. Most of the river basin sizes are well within a 20% difference of published values, with a root-mean-square error of approximately 10%. Furthermore, drainage areas for more than 400 gauging stations were delineated. Obviously, the stream lengths in TRIP are shorter than the natural lengths published as data. This is caused by the meandering of rivers in the

---

* Corresponding author address: Taikan Oki, Institute of Industrial Science, University of Tokyo, 7-22-1 Roppongi, Minato-ku, Tokyo 106-8558, Japan.

Permanent affiliation: Institute of Industrial Science, University of Tokyo, Tokyo, Japan.

E-mail address: taikan@iis.u-tokyo.ac.jp

**E-mail address: sud@climate.gsfc.nasa.gov

real world. Meandering ratio (r_M), the ratio of actual (published) river length to the idealized river length, has been calculated. Averaged globally for all available data, r_M is 1.4, although it is 1.3 for rivers with areas larger than 500,000 km². The r_M data will be useful in the design of the Scheme for Total Runoff Integrating Pathways (STRIP). In the current form, TRIP can be used as a template for producing a time series of river flow using a simple version of STRIP.

KEYWORDS: Water cycles; Geomorphology; Networks; Runoff and streamflow; Land–atmosphere interactions

1. Introduction

General circulation models (GCMs) are now becoming sufficiently realistic in simulating the rainfall, biosphere–atmosphere interactions, and land hydrology. This has been accomplished because of modern state-of-the-art land surface models are able to generate realistic evaporation and precipitation, provided the soil moisture initialization and rainfall forcing (inputs) are realistic (e.g., Oki et al., 1997). Chen et al. (Chen et al.,1997) estimated (Project for Intercomparison of Land-Surface Parameterization Schemes 2A) that the majority of flux schemes could obtain annual mean latent and sensible heat fluxes within 5 W m^{-2} of observation. This is approximately 15% of annual mean net radiation (41 W m^{-2}). The authors believe that this accuracy is quite useful for GCMs and global hydrologic models.

Since soil moisture depends upon the soil hydrology, which, in turn, involves soil water storage and runoff, it is imperative that runoff in the hydrologic model is realistically simulated. The river runoff generated in the real world must be routed through a natural network of water flow paths, such as creeks, brooks, tributaries, and major river channels. These paths are naturally created by soil erosion and are orographically modulated and temporally carved. A few exceptions represent scenarios either where humans have created new paths for water-use needs or where small passages have naturally broadened to provide cross-basin flows. In this way, these intricate river pathways become a complex network of channels and flow routes that must be accurately sorted to generate a dataset of basin-scale water channels. This dataset should largely, if not entirely, represent the streams of water runoff pathways of the real world. This provides the motivation necessary to create a database representing approximate directions of water flow, river basins, and drainage areas. We hope this dataset will be useful for evaluating the land hydrology simulated by GCMs.

All GCMs include a runoff parameterization; even though not enough attention has been paid to the simulated river discharge in global climatological studies (discharge is defined as a water flow rate through a river cross section). On the other hand, river discharge is vital for investigating climate variability and/or validating the global water balance estimated by GCMs. Indeed, errors in runoff can vitiate the soil moisture calculation and produce errors in evapotranspiration. Thus, a primary requirement of a realistic hydrologic balance is an accurate calculation of each of the component terms of the water balance.

The problem is that meteorological and climatological data on the global scales are often given as spatial (raster) data of grid points, whereas the river discharge is measured at a single location as integrated runoff in its drainage area.

Geographical information that defines drainage area for each gauging point is required in order to convert the river discharge data into spatial data or to summarize spatial data to areal mean data for the drainage area. Russell and Miller (Russell and Miller, 1990) pioneered the design and use of global templates of major river basins for hydrologic cycle studies on local as well as global scales. They converted the runoff simulated by the Goddard Institute for Space Sciences (GISS) GCM into areal mean values by a template of 2° × 2.5° grid boxes and compared them with observations.

Later, Oki et al. (Oki et al., 1992; Oki et al., 1993) used a template of 35 river basins in 2.5° × 2.5° grid boxes. Atmospheric water vapor convergence estimated from four-dimensional data assimilation products of the European Centre for Medium-Range Weather Forecasts from 1985 through 1988 were compared with observed runoff using the above template. Subsequently, Oki et al. (Oki et al., 1995a; Oki et al.,1995b) extended the analysis to 70 river basins and found that the procedure was usable for investigating and evaluating global water balance studies using river flow data from observations.

Coe et al. (Coe et al.,1995) and Levis et al. (Levis et al., 1996) used continent and ocean templates in 4.4° × 7.5° and 2° × 2° grid boxes, respectively, and examined the water budgets in their numerical simulations.

In these studies, the templates are the converters between distributed areal data, such as model generated runoff, and areal mean hydrologic data, such as river discharge.

In recent years, Vörösmarty et al. (Vörösmarty et al., 1989) prepared a river routing network for the Amazon River basin in 0.5° × 0.5° grid cells. They coupled a water balance model with a linear transfer model in river channels to simulate river discharge. Subsequently, a similar system was applied for the Zambeze River basin by Vörösmarty et al. (Vörösmarty et al., 1991). Miller et al. (Miller et al., 1994) employed a linear routing model to simulate monthly discharge based on runoff by the GISS GCM. Sausen et al. (Sausen et al., 1994) used their river routing model in approximately 5.6° × 5.6° grid boxes and simulated monthly runoff as well. Even though only for the Mississippi River basin on a 2° × 2.5° resolution, Liston et al. (Liston et al., 1994) made a river channel network and compared simulated results with observations at a few discharge stations within the basin. Kanae et al. (Kanae et al., 1995) applied the river routing model of Miller et al. (Miller et al., 1994) to GCM outputs using their river channel network with an approximate 5.6° × 5.6° resolution. Coe et al. (Coe et al., 1997) used a similar linear reservoir model in a 2° × 2° grid and coupled it to their model to predict surface waters. Costa and Foley (Costa and Foley, 1997) simulated river discharge for 56 stations in the Amazon River basin on a 0.5° × 0.5° resolution.

A continental-scale system of rivers at 0.5° × 0.5° spatial resolution was developed and used in Vörösmarty et al. (Vörösmarty et al., 1997) to estimate the mean residential time of water. The Global Soil Wetness Project has been sponsored under the International Satellite Land Surface Climatology Project

(ISLSCP) to evaluate land hydrology schemes in GCMs and to produce a reliable distribution of global soil wetness (Dirmeyer et al., 1997).

All the required atmospheric forcing data and physical parameters for land surface parameterizations (LSPs) has been provided in a set of five CD-ROMs (Meeson et al., 1995; Sellers et al., 1995) by $1° \times 1°$ grid boxes over land for a 2-yr period: 1 January 1987–31 December 1988.

Various modeling groups have run their land–biosphere schemes to simulate all components of the land hydrology. Validation efforts have included the comparison of model products with river discharge. This requires delineating a river basin and a river routing network, along with a realistic hydrologic flow scheme.

Since there has been little information about global river basins in $1° \times 1°$ grid boxes, as a first step we have produced a global river channel network on a $1° \times 1°$ resolution, hereafter known as the Total Runoff Integration Pathways (TRIP) network.

In this framework, annual and climatological water balance can be studied with a template alone, and the seasonal and monthly water balance can be examined using channel network information with a river routing model of sufficient accuracy. One of the merits of TRIP is that it is accompanied by the locations of gauging stations and their drainage areas, which is helpful for model evaluation.

Most of the previous works based on templates of coarse resolution were unable to resolve between the whole river basin and the largest drainage area of existing gauging stations in the river basin. With a $1°$ mesh, we hope to define the drainage areas more accurately for major gauging stations in each river basin on a global scale.

The procedure to develop TRIP is described in section 2; it is succeeded by the diagnostics of the obtained TRIP in section 3. Summary and applications of TRIP are discussed in section 4.

2. Development of a global river channel network

2.1. TRIP architecture

TRIP design is required to satisfy the following criteria.

1. The locations of each river basin are correct.
2. The river basin size and the drainage area to each gauging station point (GSP) are reasonably accurate.
3. The length from each grid to GSPs or to the river mouth reflects their real length.

The first requirement is obvious, because TRIP will be used to overlay various climatic data. Since most of the continents are covered by major river basins, their locations and boundaries should be realistic. The only exceptions where this becomes difficult are the regions next to arid areas, where major runoff does not occur.

The second requirement, although obvious, is nevertheless important. Using the predetermined drainage area to the GSP, discharge is converted into runoff, which has a dimension of water depth per unit time and can be easily compared

with precipitation and evapotranspiration. Therefore, the error in the drainage area directly affects the accuracy of conversion from discharge to runoff. Fortunately, the areas of major river basins have been published, and most GSPs are attributed with their drainage areas. Comparison of the areas obtained from TRIP with these values provides validation necessary for evaluation of TRIP design. This comparison also serves as a verification for the first requirement.

The last requirement is related to the application of TRIP with runoff routing models. The histogram of the length from each grid point to the GSP may have a major influence on the hydrograph formation of a large river basin. Consequently, it is desirable that the length of the river is reasonably accurate.

In constructing the water flow channel network for TRIP, each grid point was idealized to have only one outflow direction with reference to its eight neighboring grid points: N, NE, E, SE, S, SW, W, and NW. It may be classified as "D8" and its disadvantages are discussed in Costa-Cabral and Burges (Costa-Cabral and Burges, 1994). They show that statistical or partial treatment of river channel network, in which each grid may have two or more outflow grids, may be more realistic in some cases, particularly for regions with complicated boundaries. For the global domain, however, the simple format amply satisfies the requirements stated in the previous section; that is, it represents the area size adequately and relates to the lateral flow directions realistically. The numbering of direction is set 1 to 8 clockwise from north. The 0 value is used for a sea grid, and 9 is used for a "river mouth" grid defined as a grid that has no outflow to its neighboring land grids.

2.2 River flow directions in TRIP

There are two known methods of obtaining river flow directions: 1) digitizing water flow directions that can be delineated manually from published maps or 2) extracting the water path directions by a numerical analysis procedure from digital elevation models (DEMs) objectively (automatically). Even though laborious, the first method guarantees accuracy, while the second method is also bound to produce the valid results in a majority of the cases, provided that the quality of the DEM used is accurate over all the target region and the automatic algorithm is able to sort out the pathflows accurately. River channel information on Earth is already available as vector data. Dirmeyer (Dirmeyer, 1995) converted the vector information into raster data. Nevertheless, it is still helpful to extract river channel information from DEMs, because the density and quality of the existing vector data of river channels are not sufficient, as was also pointed out by Dirmeyer (Dirmeyer, 1995).

There have been earlier attempts in making a river channel network from DEMs (e.g., Tarboton et al., 1991), but most of them were applications for high-resolution situations in which DEMs were used on 1–100-m horizontal resolution. On such a small scale, automated techniques, for defining river channels, can extract detailed water flow paths on small river basins. Our goal is to create TRIP for the use in global models that have a much coarser resolution and requires resolution to capture the large-scale picture. Because of the scale difference, the following issues must be addressed.

1. Valley floors are not well represented by DEMs, because a 1° mesh corresponds to approximately 100-km horizontal resolution.
2. The treatment of "pits" or "hollows" in the continents, where the altitude of the grid box is lower than all the neighboring grid boxes, is a major problem to be dealt with. Generally these pits and hollows are artificially filled up in the DEM in order to prevent the dead ends of streams produced by automatic procedures. However, there are inland river basins on the continental scale and the dead ends of streams for such rivers are correct.
3. TRIP design should identify lakes. Some of them are inland lakes, and some of them have outlets for streams that eventually lead to the ocean. On smaller scales, generally lakes were not treated by automatic techniques, but for the larger scales lakes should be included.
4. Most of the previous studies extracted river channels for a specific river basin from DEM, but the number of river basins in TRIP is not prescribed.

Problems 1 and 2 are related to the horizontal resolution of the DEM used, while 3 and 4 are related to the target region being global. In studies of small scales, results from automated techniques were validated vis-à-vis published maps or air photos, but such a validation is not viable for TRIP, because our goal is to extract the broad features of water flow that emerges from subgrid-scale water flow structures. We believe any river channel network produced by automated techniques needs to be verified against real-world atlases, and wherever the outcome differs from the actual direction of river flow, we introduce manual correction. As a consequence, the river channel network extracted by an automated technique was viewed as a first guess, and it was modified by manual corrections to address the difference between real versus ideal world.

2.3. Automated extraction of TRIP from a DEM

To produce the first guess of TRIP, river flow directions were determined from a global DEM called ETOPO5 (Edwards, 1986). ETOPO5 has $5' \times 5'$ horizontal resolution; thus, it has 12×12 cells in each $1° \times 1°$ grid box. In each grid box, mean elevation of $5' \times 5'$ cells above 0 m was calculated and used for the extraction of river channel network. The values of medium, maximum, and minimum elevations in each 1° grid box were also prepared.

The delineation of land and sea followed the land–sea mask of the ISLSCP Initiative I CD-ROM (Meeson et al.,1995; Sellers et al.,1995). Large lakes were classified as sea in the land–sea mask, but some of them are parts of drainage systems of rivers. Therefore, such a sea grid box in the land–sea mask was changed into a land grid box, and its outflow direction was attributed during the manual correction step. Thus the lakes in current TRIP are grid boxes that have flow directions but are classified as sea in the land–sea mask of the ISLSCP Initiative I CD-ROM.

As for most D8-type river channel networks, the idea of "hydrological flow modeling method," as illustrated by Chorowicz (Chorowicz, 1992), was em-

ployed. The outflow direction was toward the lowest land point of the eight neighboring grids, provided the point was lower than the originating point. It might appear that the direction toward the steepest slope should be the obvious choice but considering that there is meandering and unevenness within the subgrid scale, it is assumed that somehow water will find a way to reach the lowest level. We shall show that the choice between steepest slope and lowest neighbor was not a clear one because both methods produced a similar number of grid cells requiring subjective correction (see section 3.2). In fact, approximately 70% of the directions determined by these two algorithms were identical. Therefore we opted for the simplest choice, that is, lowest neighbor method. If more than one outflow directions were found, the median, maximum, and minimum values of neighboring $1° \times 1°$ grid boxes were examined in this order. If a grid point was lower than all neighboring grids, it was marked as ''hollow'' and was left for the subjective evaluation and manual correction. If such a hollow grid box had a sea grid in its immediate neighborhood, it naturally became a river mouth.

Antarctica was processed differently. Lateral flow in this area is glacier flow and not river (water) flow; therefore, the river channel network merely represents internal consistency of TRIP. If ice height was lower in the grid box to the north, northeast, or northwest, outflow direction was set to that direction. In all other cases, outflow direction was set to the north.

The result obtained from the above algorithm showed fairly realistic pathways as compared to the observed pathways. Rough stream structure and the drainage system to the ocean were well represented by the automatic procedure. The hollow grids were found to be located appropriately in areas such as at marshes and lakes or at the confluence of large tributaries.

2.4. Manual correction of TRIP

A manual correction was applied to the TRIP network, obtained from the automated method, by comparison with published geographical information on water flow networks. This is done by overlaying TRIP on the actual river channels using the General Mapping Tools of Wessel and Smith (Wessel and Smith, 1995). Global continents were divided into 27 regions, and the river channel network was carefully examined and corrected. Refer to Figure 10 as an example of overlaid maps. Additional information to verify and correct TRIP was obtained from two atlases (Teikoku-Shoin,1985; Rand McNally,1995).

Some of the problems encountered in the river channel network are as follows. The first problem relates to the diversion of a river channel into two or more major streams. This is a common occurrence at a delta near the river mouth. There are only a few rivers whose deltas are resolved on a $1° \times 1°$ grid; however, when it gets resolved, it is impossible to assign the flow directions because TRIP design allows only one outflow direction. For example, this situation arose in the Amazon, the Nile, and the Lena River pathways. For all these cases, one direction of outflow was assigned as a major pathway referring to the atlases referenced above. Since there are no major gauging stations in these areas, these approximations are not likely to cause a serious problem for simulating/evaluating river flows from runoff at grid points.

Most of the other problems were encountered in arid and dry land regions. There are a number of *wadis* in dry regions, and small streams from these regions occasionally run into a main stream. It is difficult to decide whether to include such a stream flow in a major river basin, but lateral flow of water in this region would be inactive for all practical purposes and the decision of flow direction would have an inconsequential effect, particularly for GCM-scale models. Some grid boxes with inland lakes were attributed to river mouths, and river mouths are also arbitrarily put into arid areas in order to terminate water flow from mostly dry channels into episodic ponding. This is indeed realistic, but the automatic algorithm was unable to handle it appropriately.

The following features of TRIP were checked in order to correct possible inaccuracies caused by manual operations.

1. No river channels are allowed to crisscross.
2. All river channels flow from one land grid box to another.
3. Every land grid box has one, and only one, river mouth toward its downstream, which eliminates the possibility of grid boxes counterflowing toward each other.

2.5. Postprocessing of TRIP

TRIP divided the entire land into river basins. Each river mouth was given a temporary river basin number (RBN). To assign an RBN to a grid point without an RBN, the downstream grid point was examined, and the upstream grid point received the same RBN as the downstream grid point. This procedure was followed for all grid points and repeated until all the land grid points had an RBN. The chosen values of RBNs were allocated in the descending order of basin sizes. Thus, a larger river basin has a smaller RBN.

In order to demarcate the river basin boundaries, color-coded numbers were attributed to each river basin. Diagonal grid boxes were considered to be in contact and they were given different color codes if they belong to different river basins. In the current TRIP, seven colors were sufficient to distinguish adjoining river basins.

The order of streams was determined by an automated procedure. We define headwaters as the grid points with no inflow from any of their eight neighbors; the streams from the headwaters were assigned the river order of 1. The headwater grid cells were identified first, then each stream was given the grid distance from headwaters. All the grid points with 1 grid distance from the headwater grids were tested for water inflow. If two or more streams of river order 1 flow into the grid box, the outflow stream was attributed the river order of 2; otherwise, it continued to be river order 1. The confluence of two or more streams of n order produces an $(n + 1)$-order stream. All the grid boxes were examined in this way in order from the shorter grid distance to the headwaters. Because more than three tributaries can make a confluence, the river orders of all inflow streams were stored during these steps, and the river order was increased by $+1$ when the highest river order and the second highest river order were the same.

A river catalog has been prepared that identifies the river basins (see Table 1). The location of river mouth, its name, and its official river basin size are given
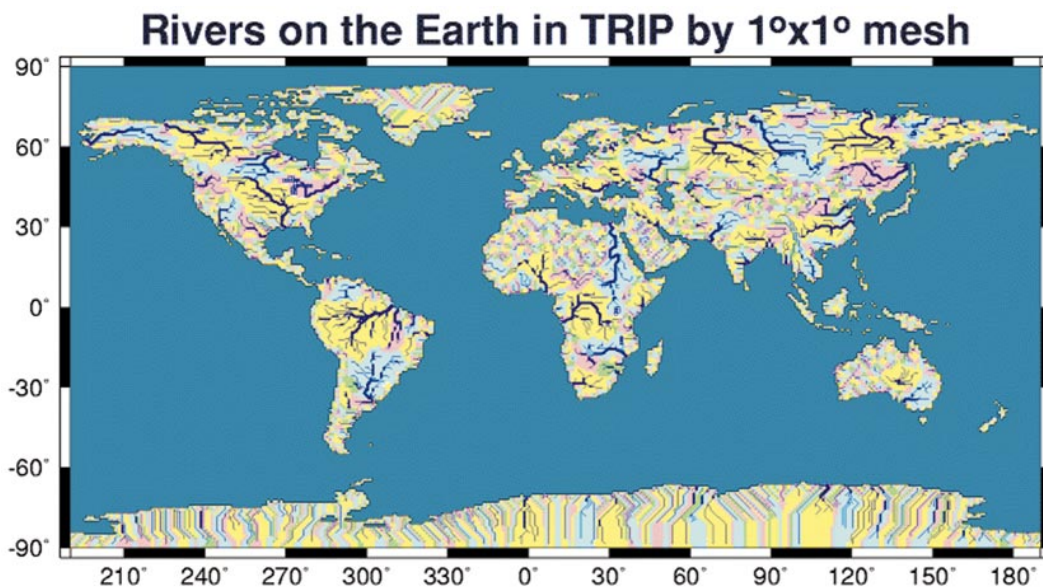
Rivers on the Earth in TRIP by 1°x1° mesh

Figure 1. Global illustration of the 1° mesh TRIP. The thickness of the line corresponds to the river order of streams, and only the streams of the order of 2 or higher are drawn.

in the catalog. Major river basins with areas larger than 100,000 km^2 are all included in this catalog. Since we recognized the possibility of estimation errors, we extracted river basins with official areas of more than 50,000 km^2 from Korzun (Korzun, 1978, hereafter referred to as KU78) and compared with the basin sizes in TRIP.

A similar catalog, but for selected gauging stations of river discharge, has been prepared as well. The selections and the locations of gauging stations are from the Global Runoff Data Centre catalog (GRDC, 1992). Some of them are from ISLSCP Initiative I datasets. Drainage area numbers were attributed to each grid point by an algorithm similar to the one used for the river basin numbering described above.

The distance between grid points was computed by an algorithm described in appendix A. The length of the stream from the grid point to its river mouth was also computed. The stream length at the grid box of the river mouth was set to zero. The longest stream length in each river basin was taken to be the representative length scale of the river basin. Indeed, that is not the case in some river basins such as the Mississippi. Itasca Lake, in Minnesota, is defined as the origin of the Mississippi River, and the length from Itasca to the river mouth, New Orleans, is approximately 3800 km. However, the Missouri River has the longer stream length, with more than 6200 km for the entire Mississippi River.
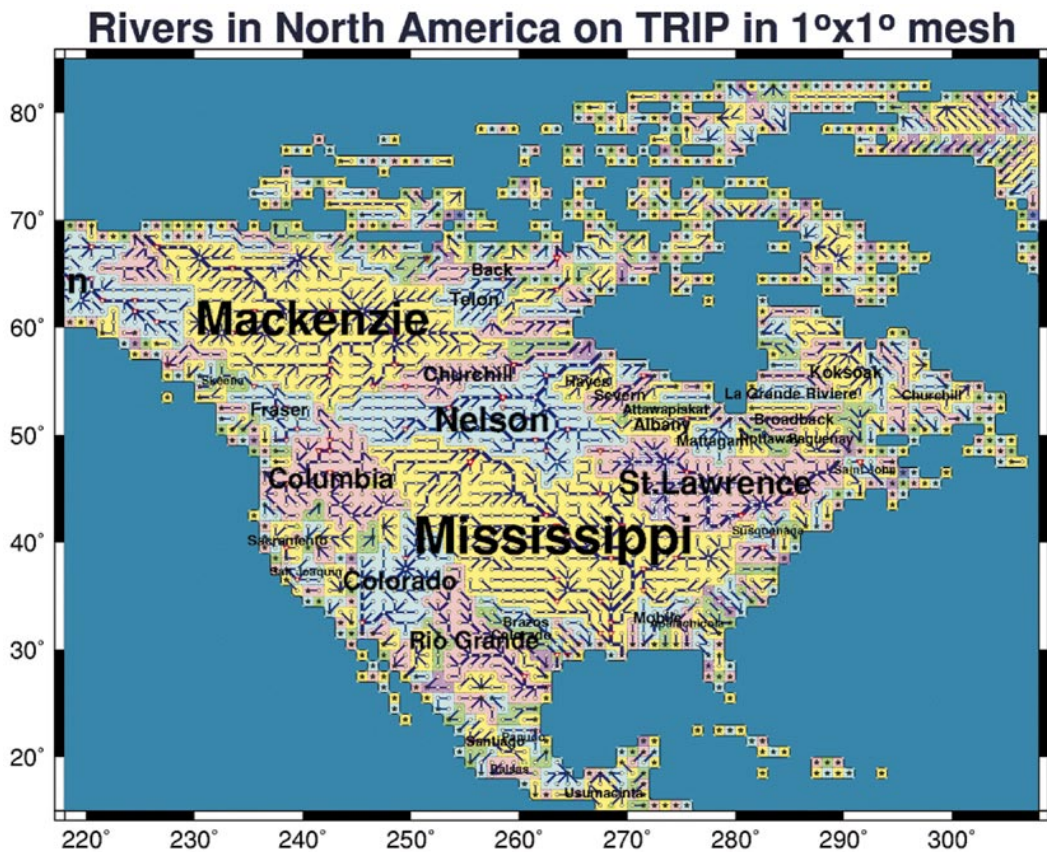
Figure 2. One-degree mesh TRIP of North America. River mouths are plotted by "★." The thickness of the line corresponds to the river order of streams. For identified rivers, the river mouth, the farthest grid from the river mouth, and the gauging stations are marked by "○," "△," and "▽," respectively. Lake grids are marked by "□."

3. Diagnostics of TRIP

3.1. Configuration

The global network invoked by TRIP is shown in Figure 1. Only the streams of the order of 2 or higher are drawn in the figure. Major drainage systems are also identified.

Figures 2–7 illustrate further details of TRIP configurations for six major continents. The thicknesses of connecting lines represent the river order of streams. The river heads, the farthest grid points from the river mouth (origin for calculating the river length), and the gauging stations of identified river basins in Table 1 are highlighted by "○," "△," and "▽," respectively. Lake grid points are overlaid by "□." A total of 3560 basins are identified in TRIP; some of them are one grid cell basins, where the river mouth grid itself is the only one in the basin.
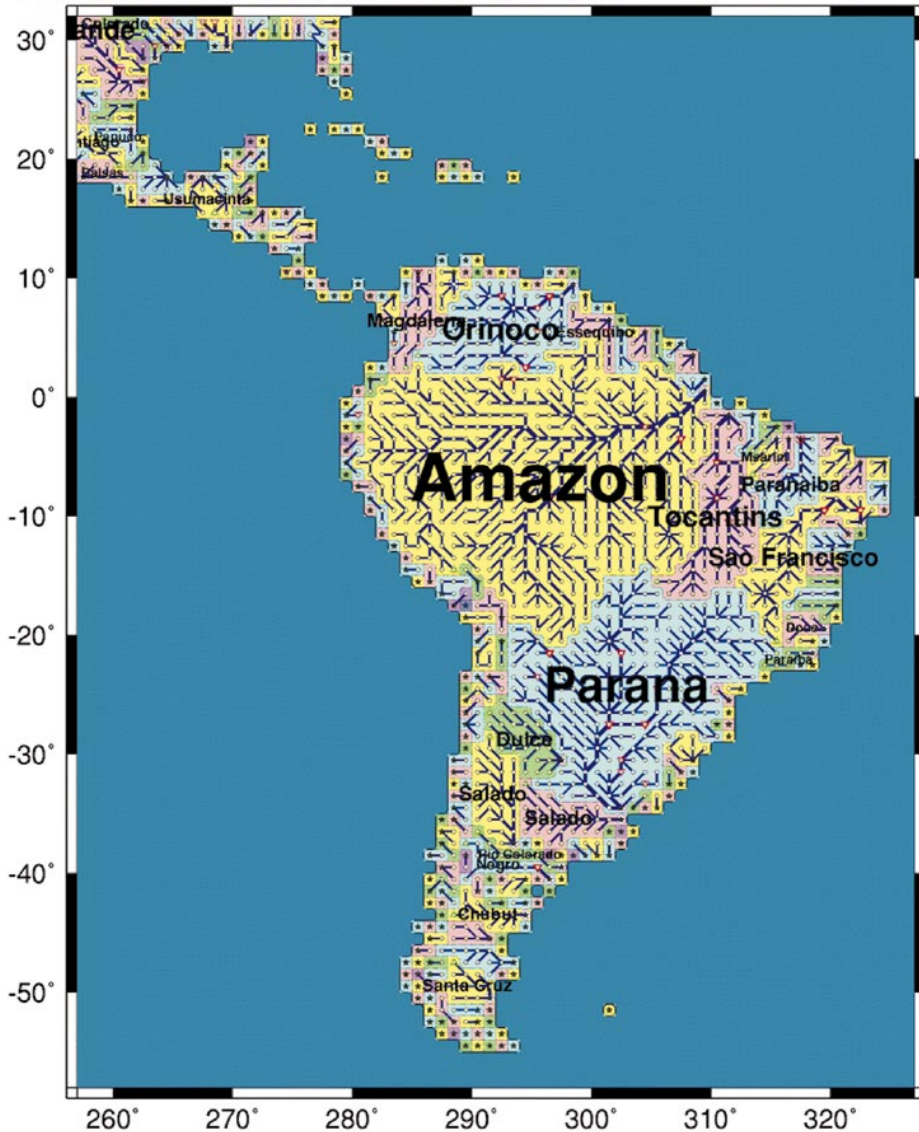
Figure 3. Same as Figure 2 but for South America.

As described in the previous section, river basins with an area larger than 100,000 km² in TRIP were identified, and the river basins with official areas over 50,000 km² are delineated; this yielded 180 rivers that are listed in Table 1. Antarctica and Greenland water flow channels are excluded; consequently, the sequential number of river basins is not continuous. Some rivers have more than two names, and representative names are shown in Table 1. The location of the river mouth is identified from atlases (Teikoku-Shoin,1985; Rand McNally,1995), but when a few river mouths happen to be close to each other in the observations,
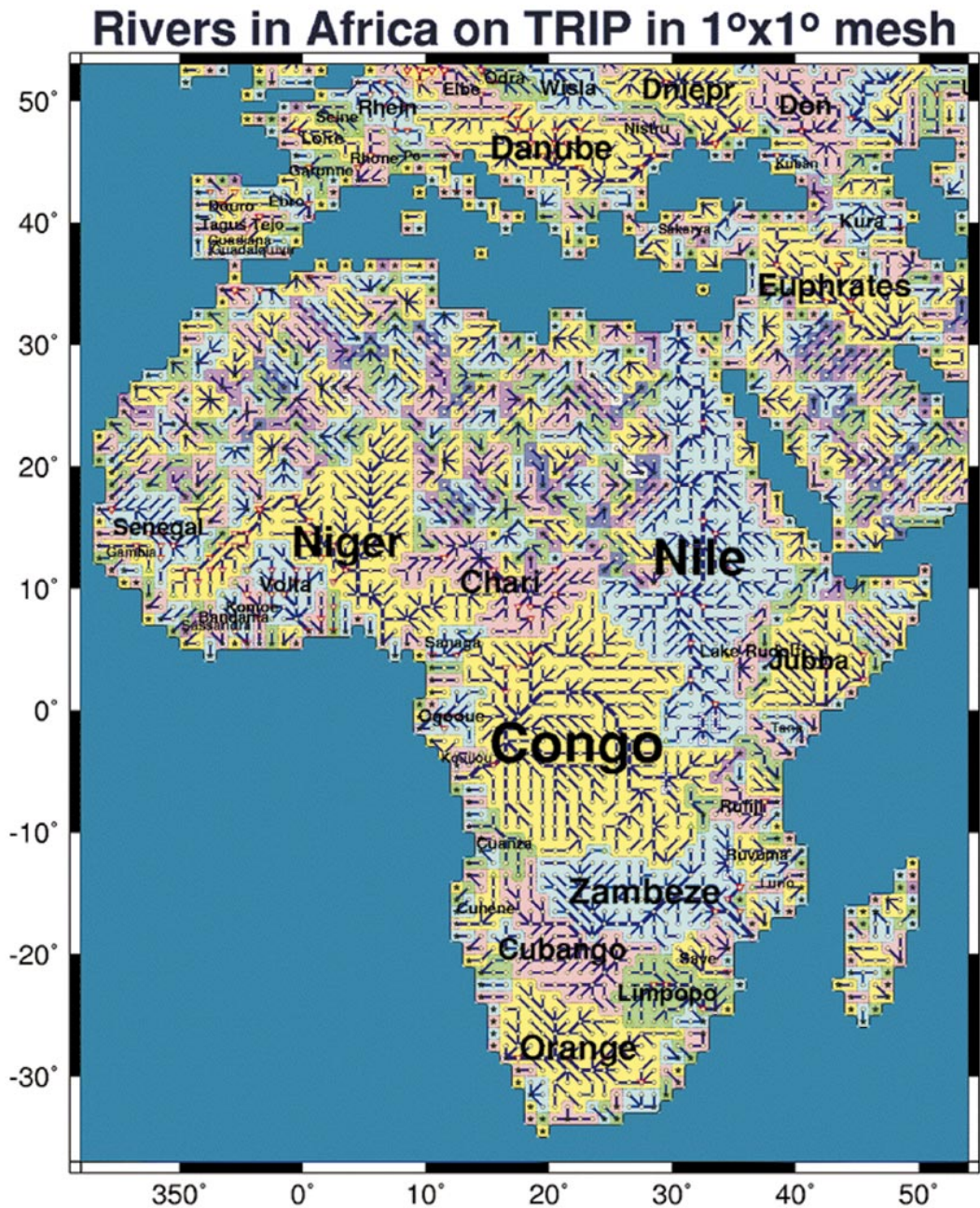
Figure 4. Same as Figure 2 but for Africa.

a $1° \times 1°$ resolution is not sufficient to resolve such details, and their locations are adjusted within plus/minus one grid box. River basin area A_T in TRIP is compared with published values A_O from Matsuyama and Oki (Matsuyama and Oki, 1992, hereafter referred to as MO92), A_K from KU78, and A_M contained in Milliman and Meade (Milliman and Meade, 1983, hereafter referred to as MM83).
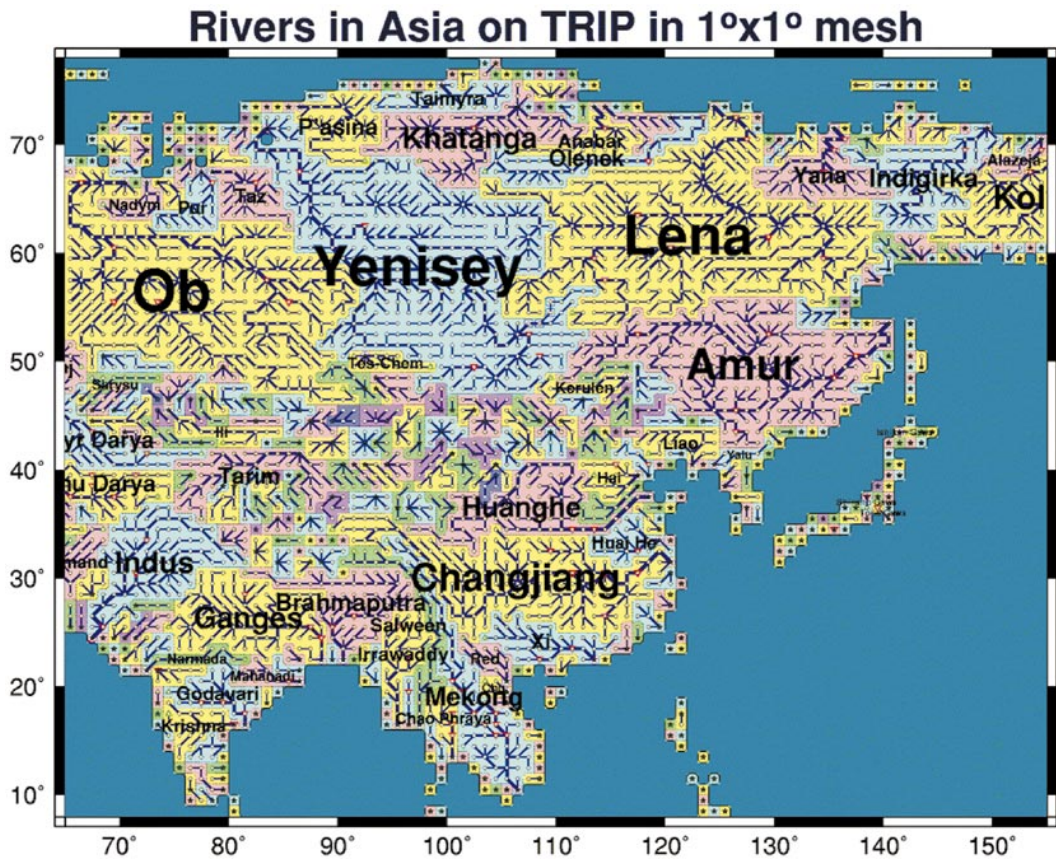
Figure 5. Same as Figure 2 but for Asia.

River length in TRIP (L_T) is compared with L_K from KU78 and L_R from the Japanese National Astronomical Observatory (Japanese National Astronomical Observatory, 1993, hereafter referred to as JNAO93). The number of $1° \times 1°$ grid boxes in each river basin is also shown in Table 1; clearly, the ratio of the number of grid boxes to basin area varies with latitude, because grid cells do not represent equal areas.

Figure 8 is the illustration of the river basins identified in Table 1. These basins cover 84×10^6 km^2 or 63% of land (excluding Antarctica and Greenland). Most of the noncovered areas are arid regions, and they have minimal influence on the global river runoff.

Figure 9 is the illustration of drainage areas for selected gauging stations. Currently, more than 400 gauging stations are available, and their own drainage areas are from less than 10,000 km^2 to more than 1,000,000 km^2. The median size is approximately 70,000 km^2, while mean size is 150,000 km^2, and the standard deviation is 300,000 km^2. Since the area of the $1° \times 1°$ grid box is approximately 10,000 km^2, the mean size of 150,000 km^2 implies that the continents are effectively divided into $4.0° \times 4.0°$ boxes. These drainage areas currently cover
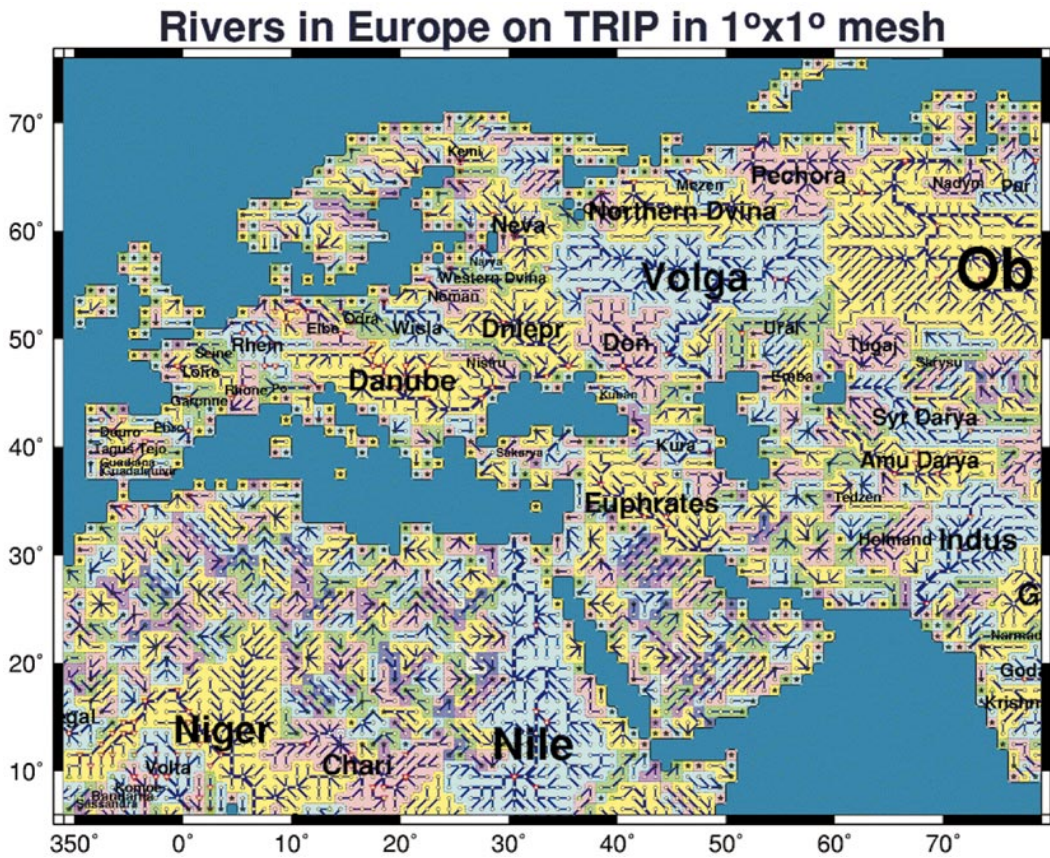
Figure 6. Same as Figure 2 but for Europe.

62×10^6 km², which corresponds to 47% of land (excluding Antarctica and Greenland). Further compilation of runoff data will increase these numbers.

3.2. Results of manual corrections

The outcome of manual correction of TRIP is summarized in Table 2a. The numbers of the grid boxes before and after the manual correction are shown. Sixty-two grid boxes were relabeled from "sea" to "land," because they contain lakes in continents on the pathways to river mouths.

Approximately half of land grid boxes are subjected to some manual correction, while the other half required no correction. The authors believe the main reason for this is the coarseness of the horizontal scale. Individual slopes and river channel valleys are not well represented in the DEM, and the actual stream flow network is not well determined by the mean topography on a $1° \times 1°$ resolution.

From past experiences in smaller scales, the steepest slope algorithm may seem appropriate for the first guess, but for our $1° \times 1°$ DEM, the steepest slope algorithm was found to produce virtually the same number of the river flow
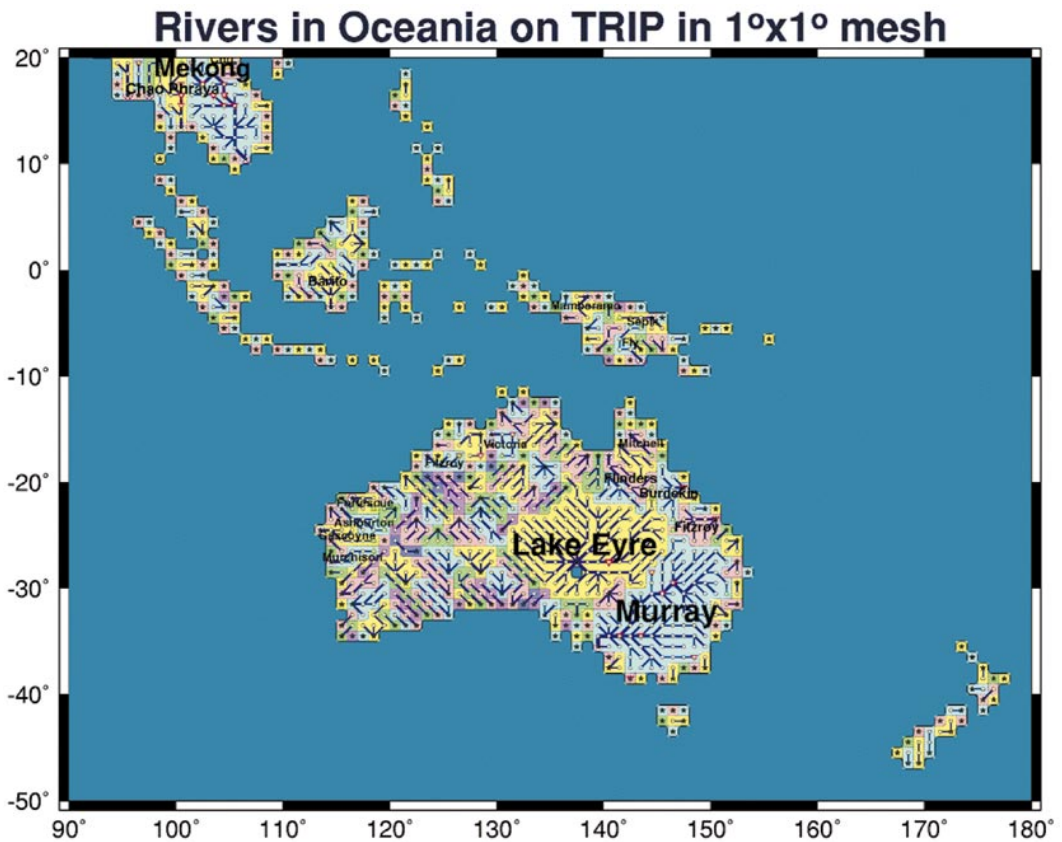
Figure 7. Same as Figure 2 but for Australia.

discrepancies as the lowest neighbor algorithm. The statistics on how many manual corrections are required for the vis-à-vis lowest neighbor algorithm are compared. The similarity can be seen between Table 2a by lowest neighbor algorithm and Table 2b by steepest slope algorithm in the numbers of ''changed'' grids and their percentage.

For example, in the Amazon River basin, the first guess by the lowest neighbor algorithm is shown in Figure 10a, and the first guess by a corresponding steepest slope algorithm is in Figure 10b. The grid boxes marked by ''□'' indicate that the flow direction of the box should be changed in order to obtain the desired pathways shown in Figure 10c. The grid boxes marked by ''H'' indicates no lower grid box was found in their neighbor, and ''T'' indicates two or more candidates were found as the outflow direction. We believe whatever may be the deficiencies of the first-guess algorithm, our manual correction process eliminates them.

3.3. Validation by area size

The comparison of river basin size from TRIP (the fifth column of Table 1) with published numbers from MO92 (the sixth column), KU78 (the seventh column),
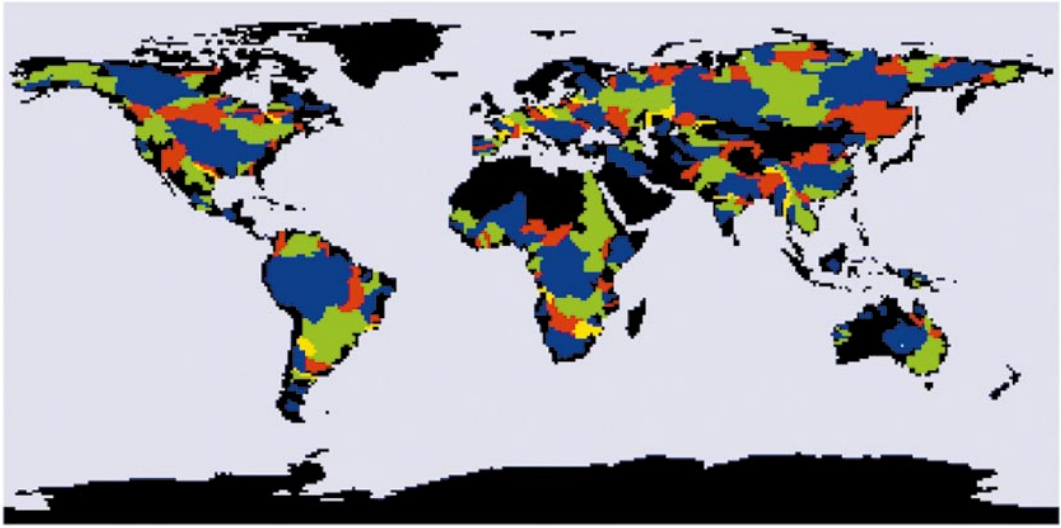
Figure 8. Coloring of identified major river basins of the globe.

and MM83 (the eighth column) is shown in Figure 11. The area of each grid cell in TRIP is a function of latitude and was calculated following the algorithm described in appendix A. MO92 compiled river basin sizes from several sources, including JNAO93. The largest drainage area of a gauging station within the river basin is sometimes substituted for the river basin area in Table 1 of MO92. Such a number is not appropriate here and is excluded from Table 1 in this paper.
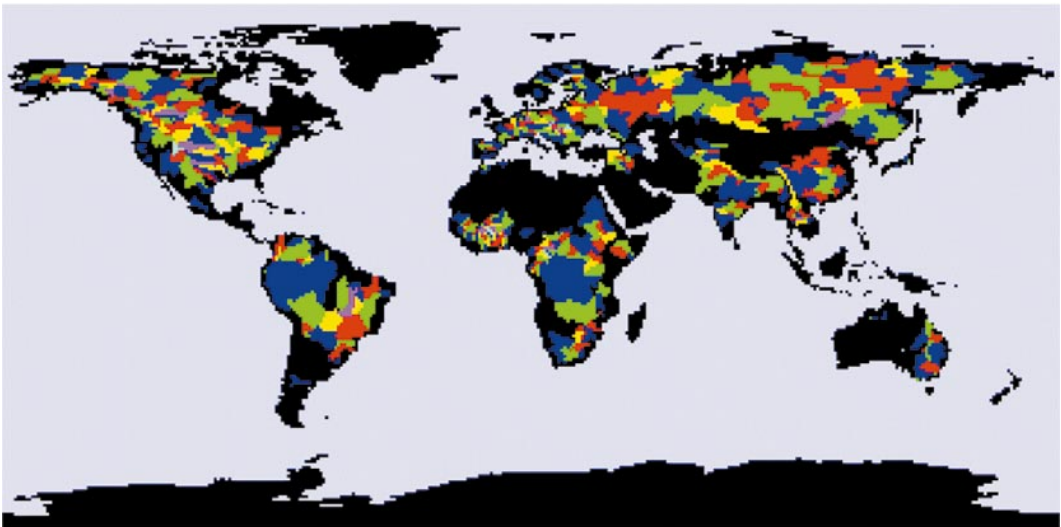
Figure 9. Coloring of drainage areas for selected gauging stations.
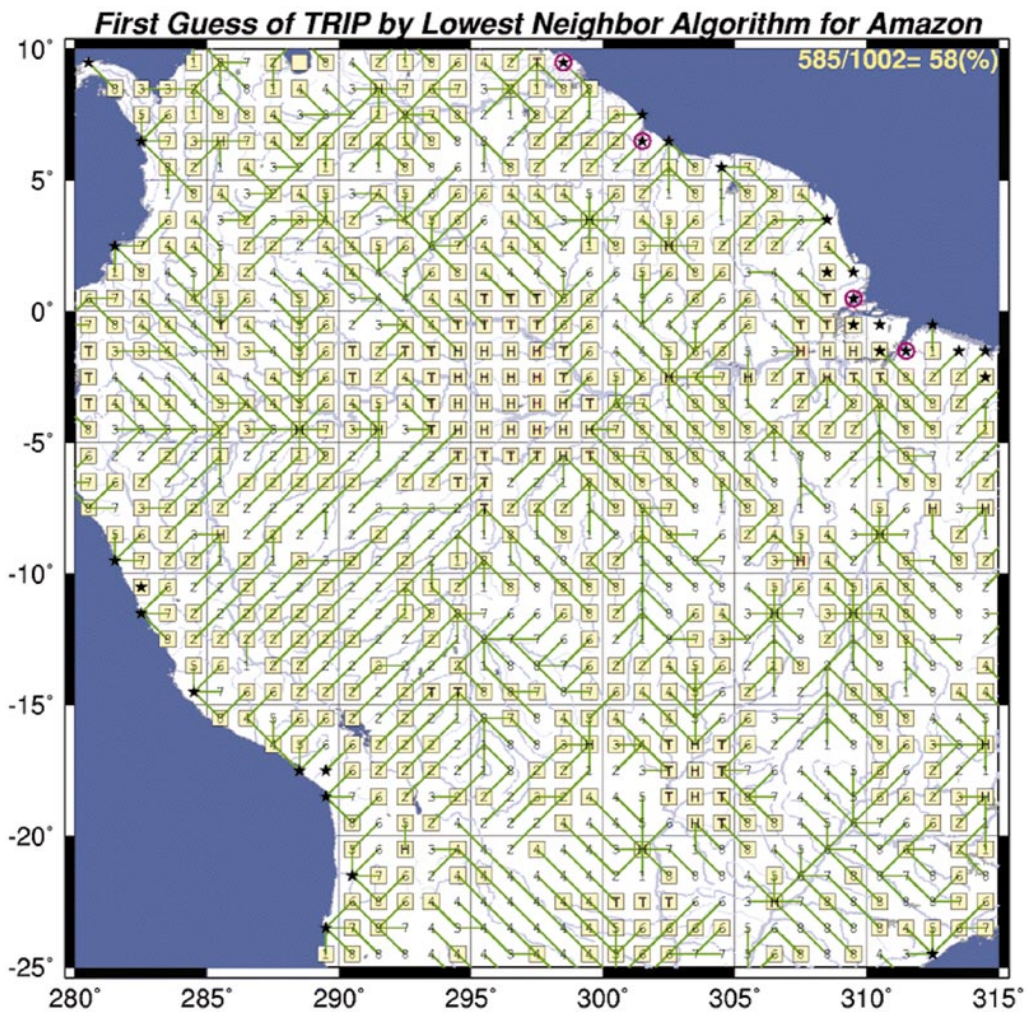
Figure 10a. First guess of TRIP in the Amazon River basin by the lowest neighbor algorithm. The grid boxes marked by "□" were changed afterward. Numbers indicate the outflow directions. Grid boxes of "H" has no outflow direction, and grid boxes of "T" has two or more candidates of outflow direction and could not decide one. Sixty-one percent of grid boxes required the correction.

KU78 included the Tocantins in the Amazon. MM83 compiled UNESCO publications, including KU78, but some of their numbers were different, especially for the Niger and the Euphrates.

According to this comparison, river basin sizes are well reproduced, but some rivers, particularly in arid regions such as the Amu-Darya and the Syr-Darya, reveal large differences vis-à-vis their official basin sizes. In fact, the corresponding values from KU78 and MO92 are also quite different from those generated by our analysis; this either may be the outcome of the specific criteria
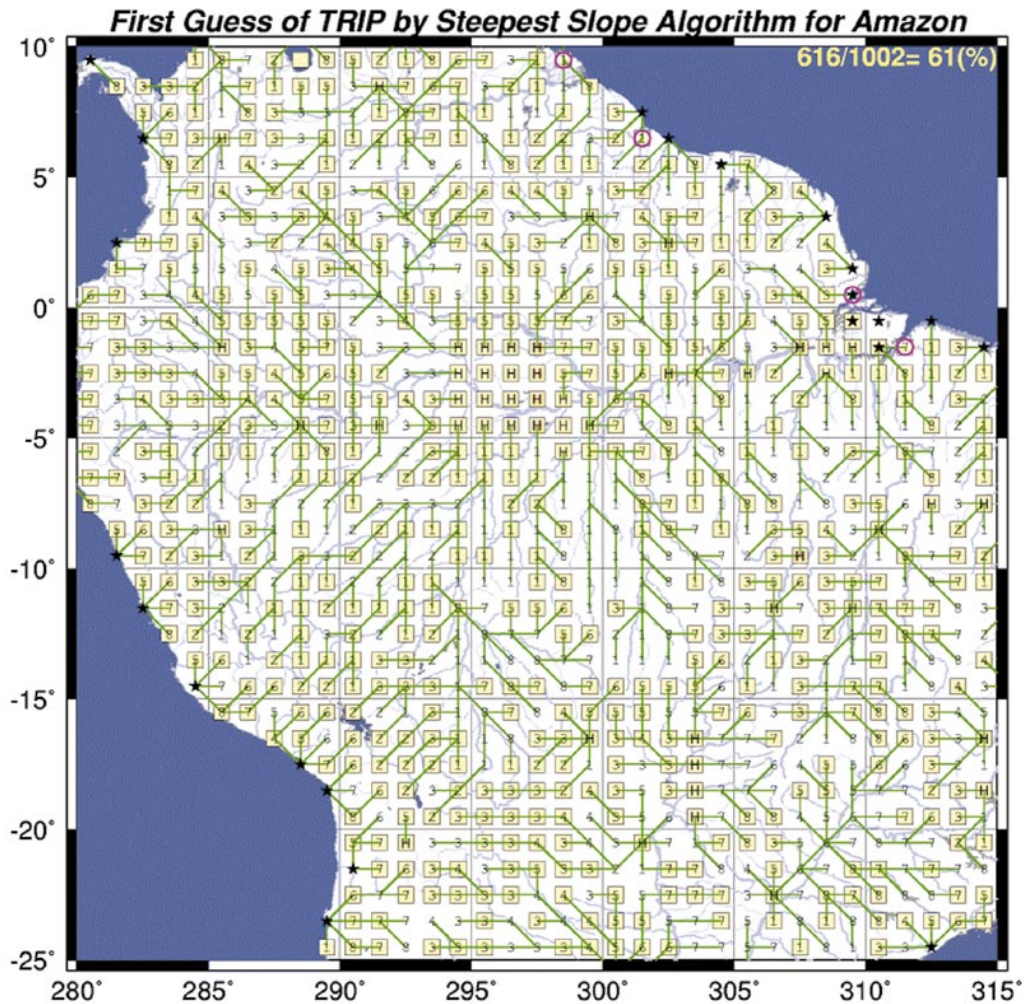
Figure 10b. Same as Figure 10a but for the steepest slope algorithm. Sixty-four percent of grid boxes required the correction.

used to define the river basin, or the official numbers may be outdated. Actually, in arid regions, there are some tributaries that connect to the main stream only when there is large runoff; for these cases, river basin boundaries where surface discharge is often inactive are unclear. Except for such cases, most of the river basins in TRIP have a difference of less than ±20% of previously published numbers. Root-mean-square errors are 11% for KU78 and MO92, and 15% for MM83.

Figure 12 compares the drainage area of more than 400 gauging stations. The area sizes in TRIP generally correspond well with official values from GRDC associated with the runoff data, even though official numbers may be inaccurate for some stations. For example, the drainage area at Tarbert Landing of the Mississippi River is 3,923,799 km^2 according to GRDC (3,052,500 km^2 in TRIP);
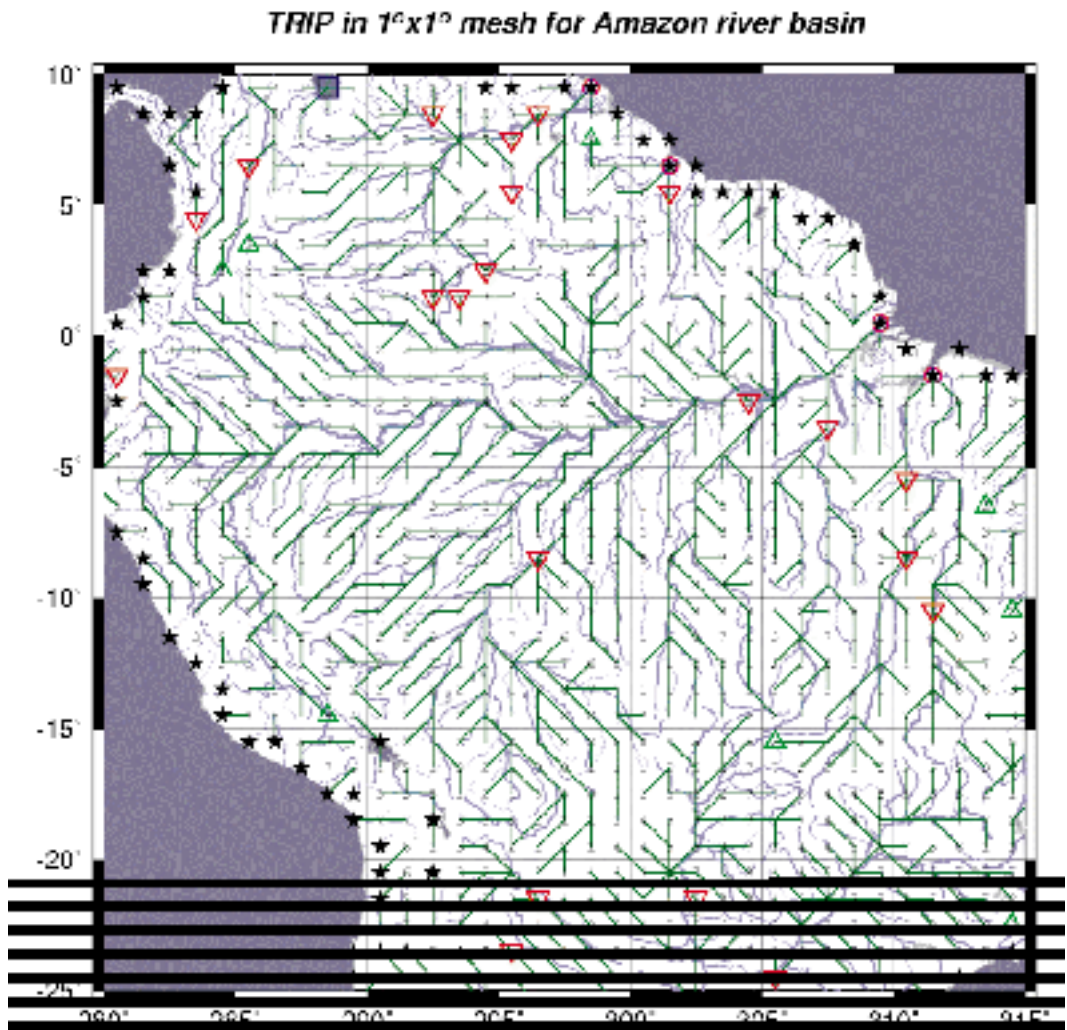
Figure 10c. Final illustration of TRIP in the Amazon River basin after the subjective improvement. Marks are the same as in Figure 2. Numbers indicate the outflow directions.

however, it is more than the total river basin area of 3,248,000 km² given by MO92. On the other hand, Matamoros is located close to the mouth of the Rio Grande (Bravo River), whose basin size is approximately 570,000 km² (610,000 km² in TRIP). It is expected that the drainage area of Matamoros is close to the basin area, but GRDC gives it a value of 450,000 km². The drainage area for Yankton, Missouri, in GRDC is 273,900 km², but it is 726,000 km² in TRIP. After an inquiry to GRDC, it was found that there was a typographical error and the correct value is 723,900 km².

Some stations in regions of lakes and marshes also have relatively large
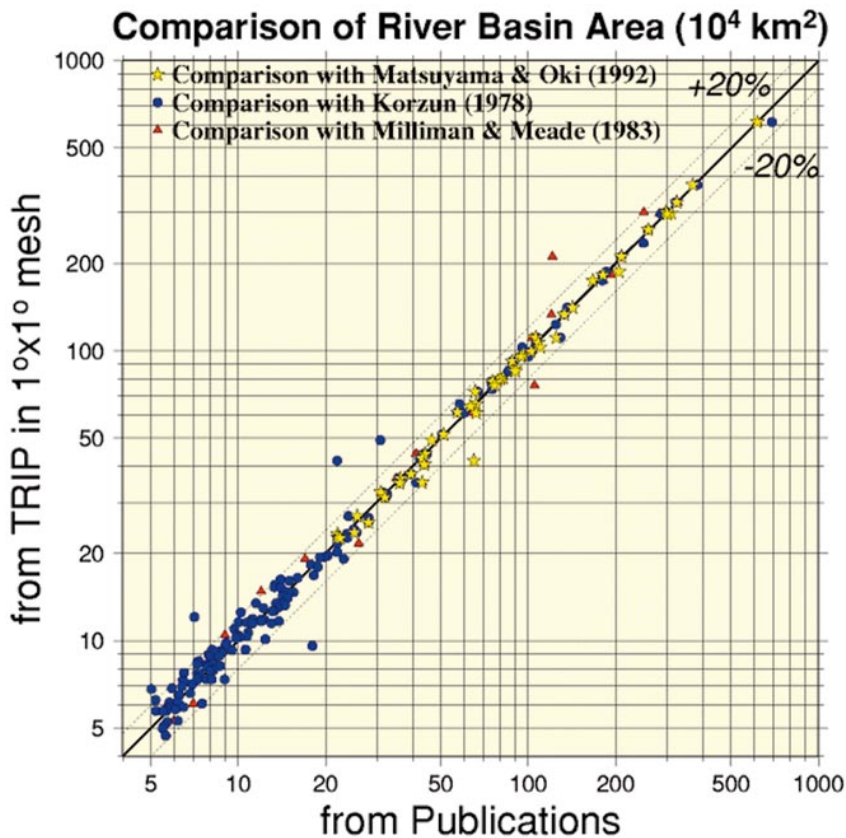
Figure 11. Major river basin areas (10^4 km²) in TRIP are compared with published numbers from MO92, KU78, and MM83. Most of the plots are within ±20% of error.

differences. In TRIP, the areas of water surface are included in the total drainage areas, but they may have been excluded in the official numbers. For example, MM83 may have excluded the area of Great Lakes from the river basin size of the St. Lawrence. In view of the above, we believe that the overall accuracy of TRIP is quite adequate for global models despite a few issues with difficult stations. The mean bias of drainage areas larger than 50×10^3 km² is 4.0×10^3 km² (1.4%) and the root-mean-square error is 67×10^3 km² (13%).

In Figure 13, the area of each river basin is plotted against its global ranking. The plot shows a linear relation between basin areas of approximately 3,000,000 km² through 100,000 km² on a log–log plot. There are two clear steps in different areas, at ranks from 12 to 13 and from 37 to 38.

3.4. Examination of river length

The longest river length in each river basin of TRIP is compared with the representative river length from KU78 and JNAO93 (Figure 14). The published river

Comparison of Drainage Area (10^4 km²)
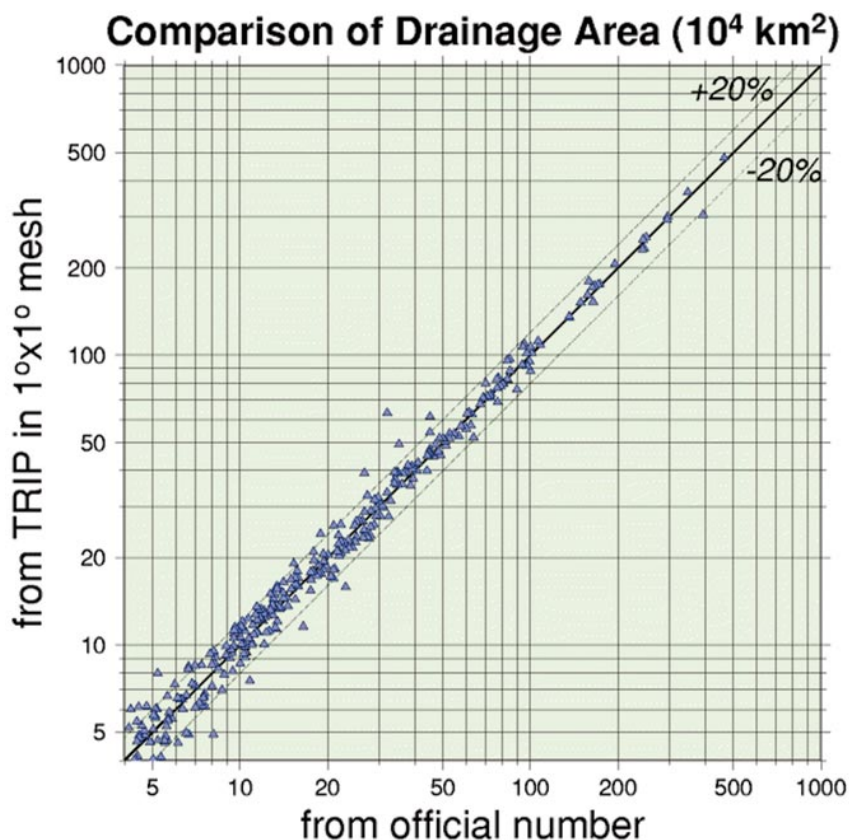
Figure 12. Drainage areas (10^4 km²) in TRIP for selected gauging stations are compared with official numbers attributed to each gauging station. Most of the plots are within ±20% of error.

length is significantly larger than that depicted in TRIP. It is mainly because the meanderings of actual river channels are a subgrid-scale feature that cannot be outlined in TRIP. Consequently, we calculate the "meandering ratio" (r_M) as the ratio of published river length to that calculated from TRIP. It represents a factor by which the stream length in TRIP must be multiplied to obtain the actual (observed) stream length. The isolines of r_M = 1.2, 1.4, and 1.6 are also drawn in Figure 14. It shows that r_M for most large rivers is close to 1.6. Large variability is seen for r_M of river basins smaller than approximately 500,000 km² (which carry rivers with a length shorter than 1500 km). This reflects not only the meandering of the stream, but the effect of idealization of the pathways of the main stream, which itself is not well reproduced in 1° × 1° resolution. The traveling time for 1500 km is of the order of 2 weeks, if the flow velocity in the streams is of the order of 1 m s^{-1}. The error in estimating traveling time, caused by the poor reproduction of stream length, can be in the 10%–25% range if such errors appear randomly. Its effect could be neglected, particularly for monthly water balance studies, but it could be crucial for flood forecasting.

River Basin Area and the Ranking
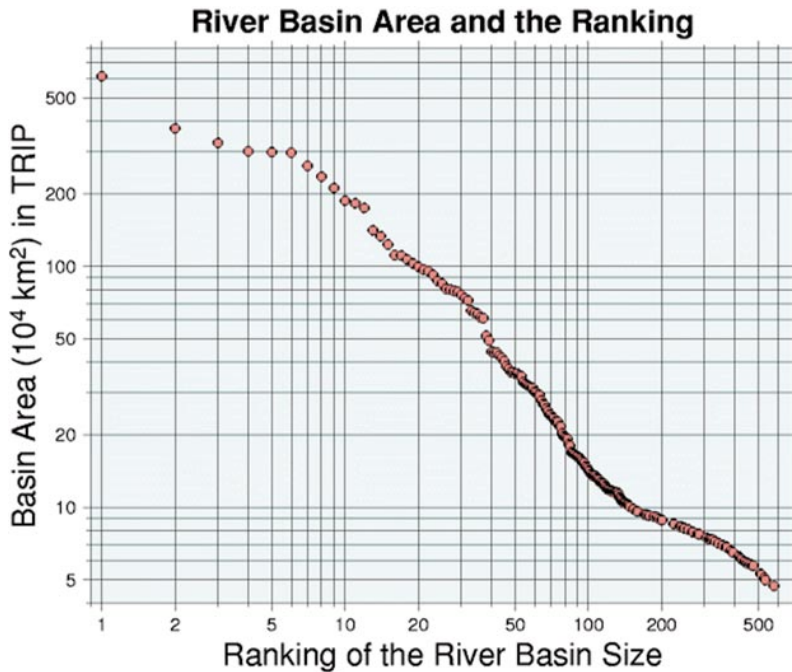
Figure 13. Ranking of area size in the globe and river basin area (10^4 km²).

The dependency of r_M on river basin size is illustrated in Figure 15. Mean r_M is plotted in each of the 200,000 (and larger than 1,000,000) km² bins. One can apply r_M depending on the area size, or use different r_M values in each river basin. Overall mean r_M of 1.4 (compared to KU78), or 1.3 for the rivers larger than 500,000 km², seem to emerge quite universally. This r_M factor can be used to apply a meandering correction as a first-order approximation.

4. Summary and discussion

A global river channel network, Total Runoff Integrating Pathways (TRIP), at 1° × 1° horizontal resolution has been constructed for the entire Earth. Its aim is to give directions for lateral water movement by creating an idealized network of river channels. First, an automatic algorithm based on grid-averaged topography was deployed to determine a "first guess" of river flow directions from a digital elevation map. Of the two possible choices, one using river outflow in the direction of lowest elevation direction and one using river outflow in the direction of steepest gradients, we adopted the first for simplicity and comparable accuracy. On comparing TRIP with the actual river channel information in atlases, we had to apply a number of subjective corrections. The TRIP map was used to prepare a template to convert the point data of river discharge into the areal data of mean runoff.

One hundred eighty rivers with more than 100,000 km² of basin area in

Comparison of River Length (km)
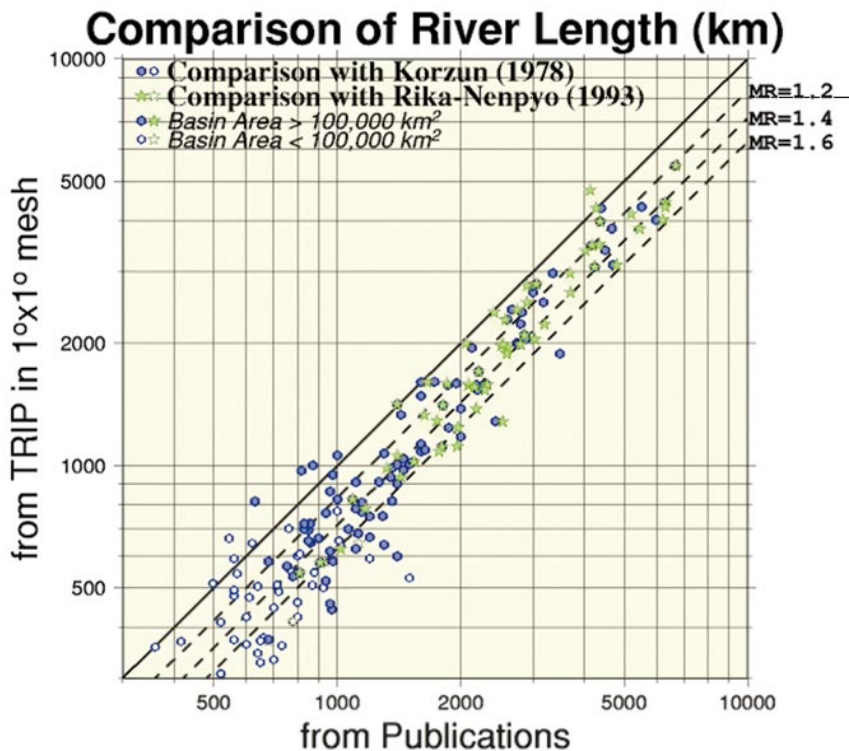
Figure 14. River lengths (km) in TRIP for major river basins are compared with published numbers from KU78 (by "●") and the Japanese National Astronomical Observatory (JNAO93) (by "★"). Rivers whose area size is larger than 10,000 km² are plotted by "●," else by "○" Most of the actual river lengths are larger than the length in TRIP.

TRIP (or more than 50,000 km², if in KU78 have been delineated. These rivers cover 63% of land (excluding Antarctica). Most of the river basin areas are within 20% of the corresponding published values (KU78; MM83; MO92).

The stream lengths in TRIP are shorter than the observed (KU78; JNAO93). More than 400 gauging stations were selected from the Global Runoff Data Centre (GRDC, 1992). Continents were divided into their own drainage basins. The size of drainage basins feeding a gauging station is well captured in TRIP. Compared with the official numbers associated with the discharge data, the areal bias in TRIP for drainage areas larger than 50×10^3 km² is roughly of the order of 4.0×10^3 km² (the mean of relative bias errors is 1.4%), and the corresponding root-mean-square error is roughly 67×10^3 km² (13%).

The stream lengths in TRIP are shorter than the observed (KU78). It is mainly because of the influence of the meandering of rivers on the subgrid scale, which TRIP cannot handle. Meandering ratio (r_M), the ratio of actual river length to the idealized pathway length in TRIP, was calculated. Averaged for all available
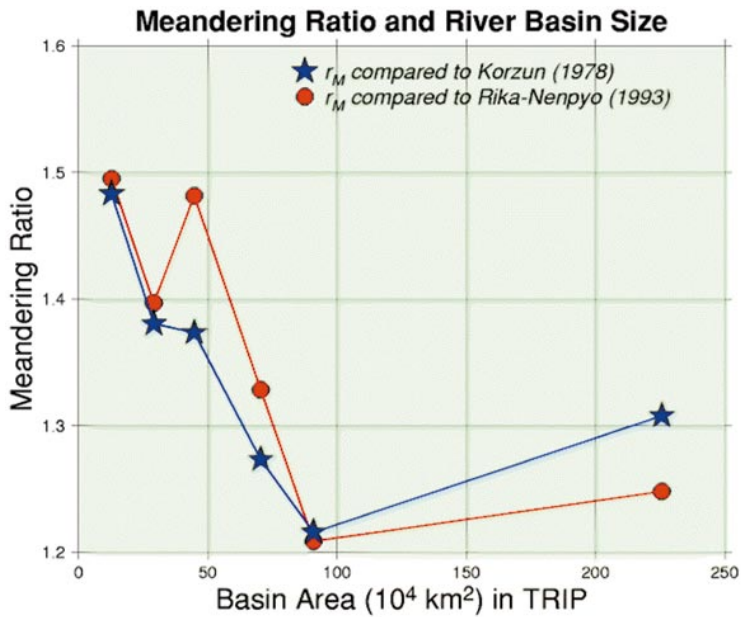
Figure 15. The dependency of r_M on river basin size. Meandering ratio r_M is estimated as the ratio of published river length from the Japanese National Astronomical Observatory (JNAO93) (by "○") or KU78 (by "★") to the longest stream length from a grid point in each river basin to the river mouth of TRIP.

data, r_M is 1.4. It is smaller for larger basins; for example, it is only 1.3 for the rivers larger than 500,000 km². All these comparisons were viable for regions where a major river exists. However, an exhaustive validation of the accuracy of TRIP could not be carried out in arid regions.

It is hoped that TRIP will contribute to several future modeling studies. Gridded runoff data can be arranged using the template of drainage areas, and it will help climatological as well as annual water balance studies. Oki et al. (Oki et al., 1997) show that the standard deviation of annual runoff error estimated by various land surface models were approximately 100 mm yr⁻¹. Since observed precipitation is the forcing data in the numerical experiments, the standard deviation of evapotranspiration has the same standard deviation error. Mean annual evapotranspiration over the globe is approximately 600 mm yr⁻¹; therefore 100 mm yr⁻¹ corresponds to approximately 17% of error. This accuracy is something we need to evaluate further and improve upon. Several LSP modeling groups are involved with improving upon the accuracy of simulated evapotranspiration and runoff. Indeed, if the main objective is to simulate the runoff in the river, one requires better accuracies with lower standard deviation. Evidently, for hydrological evaluation of models as well as real hydrological data analysis, we still have a long way to go.

Combining TRIP with a river routing model will help to evaluate LSPs of

GCMs, particularly the water balance of major rivers in a seasonal to monthly basis. We believe that inclusion of river routing in a GCM using information such as TRIP is very important when water availability and use for irrigation is an issue; in these situations, soil moisture downstream is affected by the runoff from upstream. TRIP will provide the necessary information for the better modeling of the global hydrological cycle, as well as in helping to integrate the water balance of the atmosphere, the land, and the ocean. TRIP will also be used for the on-line coupling of river routing models with GCMs; this will help to close the water cycle in GCMs. Off-line testing of a linear routing model with TRIP has been already applied and a better model, called the Scheme for Total Runoff Integrating Pathways (STRIP), is under development. Invoking a linear routing model of Miller (Miller et al.,1994) using the current TRIP dataset was employed by Oki (Oki, 1997); the model was successful in simulating the behavior of the annual cycle of the rivers identified in the TRIP design. Our more sophisticated scheme for TRIP (called STRIP) is currently under development. It is being designed to better represent the hydraulics of river flow and surface water storages. TRIP information in digital form is attached to this manuscript (Appendix B).

Appendix A: Calculating the Area and the Length on Earth's Surface

The area for various grid cells was calculated assuming Earth to be a spheroid in the meridional plane. The assumption of a perfect sphere has systematic biases of overestimation areas in the Tropics, and underestimation areas in polar regions. Discharge is generally large in the Tropics and runoff per unit area may be underestimated by the overestimation of the area size, and vice versa in polar regions. As a result, global mean runoff may be slightly underestimated. The ellipticity of the equator, however, was ignored; it is less than that of meridians in the order of 2–3.

A.1. Area size per longitude

From the table of ''Rika-Nenpyo'' (meaning ''scientific charts'' in Japanese; JNAO93) the length of the latitudinal arc (l_x) and the meridional arc (l_y) per unit angle are given as

$$l_x = \frac{a\,\cos\phi}{(1 - e^2\,\sin^2\phi)^{1/2}}$$

$$l_x = \frac{a\,\cos\phi}{(1 - e^2\,\sin^2\phi)^{1/2}} \tag{A1}$$

and

$$l_y = \frac{a(1 - e^2)}{(1 - e^2\,\sin^2\phi)^{3/2}}$$

$$l_y = \frac{a(1 - e^2)}{(1 - e^2\,\sin^2\phi)^{3/2}}, \tag{A2}$$

where a is the equatorial radius of Earth, ϕ is the latitude, and e is the ellipticalness. From (A1) and (A2), the surface area from latitude ϕ_1 to ϕ_2 per $1°$ in longitude, $S(\phi_1,\phi_2)$, can be obtained from the equation

$$S(\phi_1,\phi_1) = \int_{\phi_1}^{\phi_2} \frac{\pi}{180}\, l_x l_y\, d\phi = \frac{\pi a^2(1 - e^2)}{180} \int_{\phi_1}^{\phi_2} \frac{\cos\phi\, d\phi}{(1 - e^2\,\sin^2\phi)^2}. \tag{A3}$$

Substituting $\sin\theta = e\,\sin\phi$ in (A3),

$$S(\phi_1,\phi_1) = \frac{\pi a^2(1 - e^2)}{180e} \int_{\theta_1}^{\theta_2} \frac{d\theta}{\cos^3\theta} \tag{A4}$$

is obtained, where $\theta_1 = e\,\sin\phi_1$ and $\theta_1 = e\,\sin\phi_1$. Since,

$$\int \frac{d\theta}{\cos^3\theta} = \int \left(\frac{1}{\cos^3\theta} - \frac{1}{2\,\cos\theta} \right) d\theta + \frac{1}{2} \int \frac{d\theta}{\cos\theta}$$

$$= \frac{1}{2}\frac{\sin\theta}{1 - \sin^2\theta} + \frac{1}{4} \log \left| \frac{1 + \sin\theta}{1 - \sin\theta} \right|, \tag{A5}$$

$$S(\phi_1,\phi_1) = \frac{\pi a^2(1 - e^2)}{180e} \left(\frac{1}{2}\frac{e\,\sin\phi}{1 - e^2\,\sin^2\phi} + \frac{1}{4} \log \left| \frac{1 + e\,\sin\phi}{1 - e\,\sin\phi} \right| \right). \tag{A6}$$

For $a = 6378.136$ (km) and $e^2 = 0.00669447$, surface area from latitude ϕ_1 to ϕ_2 per $1°$ in latitude can be calculated from (A6).

The values calculated from (A6) are compared in Figure A1, with other estimates such as Baumgartner and Reichel (Baumgartner and Reichel,1975), Bryan and Oort (Bryan and Oort,1984), and the "gridarea.grz" file on the ISLSCP CD-ROM (Meeson et al.,1995; Sellers et al.,1995). The curves indicate the relative difference (%) of the area size at each $5°$ latitudinal zone compared to the estimates by this algorithm. The difference, if the area sizes are calculated assuming that Earth is a perfect sphere with the actual radius of the equator (= 6378 km), is also shown in Figure A1. It was found that the area sizes in the ISLSCP CD-ROM and by Bryan and Oort (Bryan and Oort,1984) correspond to the area sizes that were calculated with the perfect sphere assumption using radii equal to 6371 and 6366 km, respectively. The radius of 6371 km may be derived
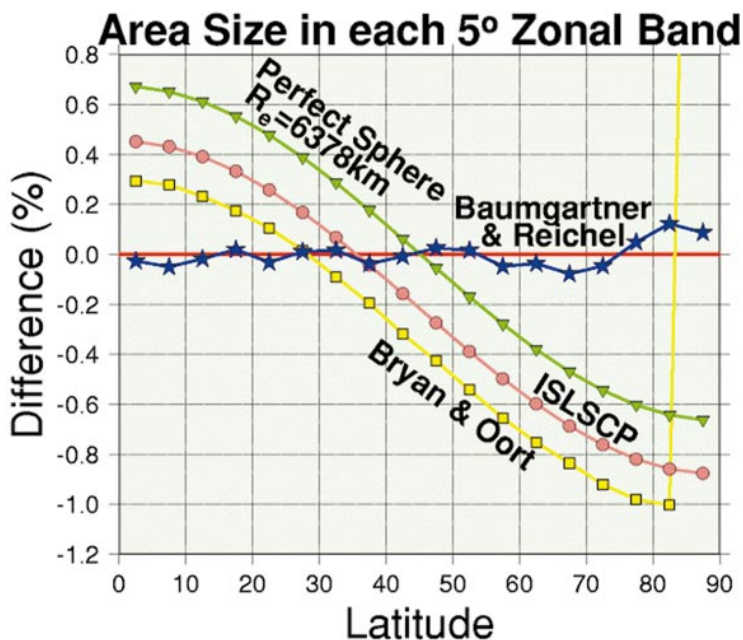
Figure A1. Comparison of the area size at each 5° latitudinal zone. The difference error compared to the values used in this study are presented. Previous studies except for Baungartner and Reichel (Baumgartner and Reichel,1975) have systematic biases in latitude.

inversely from the whole Earth's surface area of 510×10^{12} m². The radius of 6366 km is close to the mean of the equatorial and the polar radii. Residual to the total of 510×10^{12} m² might be allocated to polar regions, and that may be the reason why the area by Bryan and Oort (Bryan and Oort,1984) at 85°–90° is larger than the others. Baumgartner and Reichel (Baumgartner and Reichel,1975) have considered the ellipticity of Earth, and their estimate is very close to the result of this study as seen from Figure A1.

A.2. Surface distance

As stated earlier, the river channel length in TRIP can be expected to be shorter than observed. Therefore, a relatively simple algorithm was used to calculate the length between two grid points in TRIP.

The distance between grids is obtained from (A1) and (A2), respectively, if their latitudes or longitudes are the same. Otherwise, the distance L, between $P(\lambda_1, \phi_1)$ and $Q(\lambda_2, \phi_2)$, was calculated assuming that Earth is a sphere with an effective radius of R_e at latitude $\phi_h = (\phi_1 + \phi_2)/2$.

From the law of cosines on a sphere,

$$\cos a = \cos b \cos c + \sin b \sin c \cos A, \qquad (A7)$$

where A is an interior angle, and a, b, and c are the length of opposite sides

measured in radians. Let b and c be the longitudinal and latitudinal directions, and A makes a right angle, then $\cos A = 0$. The distance $L = a$ is obtained by

$$L = \arccos[\cos(l_x/R_e) \, \cos(l_y/R_e)] \, R_e, \qquad (A8)$$

where l_x and l_y are from (A1) and (A2). The effective radius of the earth at the latitude ϕ_h, R_e, is given by

$$R_e = N \, (1 - 2e^2 \, \sin\phi_h + e^4 \, \sin^2\phi_h \,)^{1/2} \qquad (A10)$$

$$N = a(1 - e^2 \, \sin^2\phi_h)^{-1/2} \qquad (A11)$$

The results obtained from the above algorithm would be accurate enough for TRIP, because the distances are calculated piecewise between neighbors of $1°$ grids.

Appendix B: TRIP Information

TRIP data and its derivative information are attached with this manuscript.

B.1. TRIP data

Each $1° \times 1°$ grid box is allocated a number that indicates the outflow direction from the grid box. Each grid box can have one outflow direction from eight candidates: 1) north, 2) northeast, 3) east, 4) southeast, 5) south, 6) southwest, 7) west, and 8) northwest.

Missing value, indicating that grid point is water surface, is 0. The value "9" implies that no outlet from that grid point to any neighboring land grids. It could be a river mouth.

TRIP data are provided in several formats.

B.1.1. Binary format

Four-byte real of 360×180 data are written from ($89.5°$N, $0.5°$E) to ($-89.5°$N, $359.5°$E). The following program will read the binary data file of TRIP.

```
integer i, j
real trip(360, 180)
open(15, file='trip.bin', access='DIRECT'
$    , recl=4*360, form='UNFORMATTED')
do j = 1, 180
     read (infile, rec=j) (trip(i, j), i = 1, 360)
end do
close (15)
```

The longitude (`rlon`) and latitude (`rlat`) for "`trip(i,j)`" can be calculated as

```
rlon = real(i) − 0.5
rlat = 90.5 − real(j).
```

The datafile "data1.zip" can be downloaded from the online version of this paper.

B.1.2. Two-byte integer file

The program below will read the binary data file.

```
integer i, j
integer*2 i2trip(360, 180)
open(15, file='trip.i2', access='DIRECT'
$    , recl=2*360, form='UNFORMATTED')
do j = 1, 180
    read (infile, rec=j) (i2trip(i, j), i = 1, 360)
end do
close (15)
```

The datafile "data2.zip" can be downloaded from the online version of this paper.

B.1.3. Text format

TRIP information is stored in a text file of 360 column by 180 lines from (89.5°N, 0.5°E) to (−89.5°N, 359.5°E). The "+" is used for "9," and "." is used for "0." The datafile "data3.zip" can be downloaded from the online version of this paper.

B.1.4. ASCII data

TRIP information is indicated by a line for each grid point over land. Each line has longitude, latitude, and the TRIP direction number. The datafile "data4.zip" can be downloaded from the online version of this paper.

B.2. Templates of major river basins in TRIP

Approximately 200 major river basins are delineated in TRIP. Data in the index file (data5.dat) indicate the correspondences between the river basin numbers and the river names. The longitude and the latitude of the river mouth in TRIP are presented as well. The datafile "data5.zip" can be downloaded from the online version of this paper.

The river basin number may change in the future version of TRIP and one must use the corresponding version of the index file. River basin numbers are given in the following formats. Data can be read by the same manner as in the previous section. A 4-byte real binary datafile, "data6.zip," can be downloaded from the online version of this paper. A 2-byte integer binary datafile, "data7.zip," can be downloaded from the online version of this paper. An ASCII datafile, "data8.zip," can be downloaded from the online version of this paper.

B.3. Vector data of basin boundaries of major rivers

Information on river basin boundaries is extracted from the current version of TRIP in vector format (data9.tar). The datafile "data9.tar" can be downloaded from the online version of this paper.

References

Baumgartner, F. and E. Reichel. 1975. The World Water Balance: Mean Annual Global, Continental and Maritime Precipitation, Evaporation and Runoff. Ordenbourg, Munich, 179 pp.

Bryan, F. and A. Oort. 1984. Seasonal variation of the global water balance based on aerological data. *J. Geophys. Res,* **89**,11 717–730.

Chen, T. H., A. Henderson-Sellers, P. C. D. Milly, A. J Pitman, A. C. M. Beljaars, J. Polcher, F. Abramopoulos, A. Boone, S. Chang, F. Chen, Y. Dai, C. E. Desborough, R. E. Dickinson, L. Dümenil, M. Ek, J. R. Garratt, N. Gedney, Y. M. Gusev, J. Kim, R. Koster, E. A. Kowalczyk, K. Laval, J. Lean, D. Lettenmaier, X. Liang, J.-F. Mahfouf, H.-T. Mengelkamp, K. Mitchell, O. N. Nasonova, J. Noilhan, A. Robock, C. Rosenzwig, J. Schaake, C. A. Schlosser, J.-P. Schulz, Y. Shao, A. B. Shmakin, D. L. Verseghy, P. Wetzel, E. F. Wood, and Y. Xue. 1997. Cabauw experimental results from the Project for Intercomparison of Land-Surface Parameterization Schemes. *J. Climate,* **10**, 1194–1215.

Chorowicz, J., C. Ichoku, S. Riazanoff, Y.-J. Kim, and B. Cervelle. 1992. A combined algorithm for automated drainage network extraction. *Water Res,* **28**, 1293–1302.

Coe, M. T. 1995. The hydrologic cycle of major continental drainage and ocean basins: A simulation of the modern and mid-Holocene conditions and a comparison with observations. *J. Climate,* **8**, 535–543.

Coe, M. T. 1997. Simulating continental surface waters: An application to Holocene northern Africa. *J. Climate,* **10**, 1680–1689.

Costa, M. H. and J. A. Foley. 1997. The water balance of the Amazon basin: Dependence on vegetation cover and canopy conductance. *J. Geophys. Res,* **102**, 973–989.

Costa-Cabral, M. C. and S. J. Burges. 1994. Digital elevation model networks (DAEMON): A model of flow over hillslopes for computation of contributing and dispersal areas. *Water Res,* **30**, 1681–1692.

Dirmeyer, P. A. 1995. An objective river routing scheme for runoff models. *Proc. Conf. on Hydrology,* Dallas, TX, Amer. Meteor. Soc. 91–92.

Dirmeyer, P. A. 1997. The Global Soil Wetness Project. *GEWEX News,* **7**, 3–6.

Edwards, M. H. 1986. Digital image processing of local and global bathymetric data. M.S. thesis, Department of Earth and Planetary Sciences, Washington University, St. Louis, MO, 106 pp.

GRDC. 1992. Second Workshop on the Global Runoff Data Centre. Rep. 1 Federal Institute of Hydrology, Koblenz, Germany, 96 pp. [Available from GRDC, Kaiserin Augusta-Anlagen 15–17, Koblenz 56068, Germany.].

Japanese National Astronomical Observatory. 1993. Rika-Nenpyo (Scientific Charts). Maruzen, Tokyo,.

Kanae, S., K. Nishio, T. Oki, and K. Musiake. 1995. Hydrograph estimations by flow routing modelling from AGCM output in major basins of the world (in Japanese with English abstract). *Ann. J. Hydraul. Eng,* **39**, 97–102.

Korzun, V. I. 1978. World Water Balance and Water Resources of the Earth. Vol. 25, Studies and Reports in Hydrology, UNESCO, 587 pp.

Levis, S., T. Coe, and J. A. Foley. 1996. Hydrologic budget of a land surface model: A global application. *J. Geophys. Res,* **101 (D12)**, 921–930.

Liston, G. E., Y. C. Sud, and E. F. Wood. 1994. Evaluating GCM land surface hydrology parameterizations by computing river discharges using a runoff routing model: Application to the Mississippi Basin. *J. Appl. Meteor,* **33**, 394–405.

Matsuyama, H. and T. Oki. 1992. GRDC and the runoff data (in Japanese). *J. Jpn. Soc. Hydrol. Water Res,* **5**, 65–70.

Meeson, B. W., F. E. Corprew, J. M. P. McManus, D. M. Myers, J. W. Closs, K.-J. Sun, D. J. Sunday, and P. J. Sellers. 1995. ISLSCP Initiative I —Global Data Sets for Land–Atmo-

sphere Models, 1987–1988. NASA, published on CD-ROM (USA_NASA_GDAAC_ISLSCP_001-USA_NASA_GDAAC_ISLSCP_005).

Miller, J. R., G. L. Russell, and G. Caliri. 1994. Continental-scale river flow in climate models. *J. Climate,* **7**, 914–928.

Milliman, J. D. and R. H. Meade. 1983. World-wide delivery of river sediment to the oceans. *J. Geol,* **91**, 1–21.

Oki, T. 1997. Validating the runoff from LSP-SVAT models using a global river routing network by one degree mesh. *Preprints, 13th Conf. on Hydrology,* Long Beach, CA, Amer. Meteor. Soc. 319–322.

Oki, T., K. Musiake, and K. Masuda. 1992. Estimation of global annual river runoff based on atmospheric water balance (in Japanese with English abstract). *Proc. 36th Japanese Conf. on Hydraulics,* Tokyo, Japan, Japanese Society of Civil Engineers 573–578.

Oki, T., K. Musiake, K. Masuda, and H. Matsuyama. 1993. Global runoff estimation by atmospheric water balance using ECMWF data set. *Macroscale Modelling of the Hydrosphere,* W. B. Wilkinson, IAHS, IAHS Publ. No. 214, 163–171.

Oki, T., K. Musiake, H. atsuyama, and K. Masuda. 1995a. Atmospheric water balance and global hydrological cycle (in Japanese with English abstract). *J. Hydraul., Coastal Environ. Eng,* **521/II-32**, 13–27.

Oki, T., K. Musiake, H. Matsuyama, and K. Masuda. 1995b. Global atmospheric water balance and runoff from large river basins. *Hydrol. Process,* **9**, 655–678.

Oki, T., T. Nishimura, and P. Dirmeyer. 1997. Validating estimates of land surface parameterizations by annual discharge using total runoff integrating pathways. *J. Jpn. Soc. Hydrol. Water Res,* **9**, 416–425.

Rand McNally. 1995. The New International Atlas. Twenty-Fifth Anniversary Edition, Rand McNally, 320 pp.

Russell, G. L. and J. R. Miller. 1990. Global river runoff calculated from a global atmospheric general circulation model. *J. Hydrol,* **117**, 241–254.

Sausen, R., S. Schubert, and L. Dümenil. 1994. A model of river runoff for use in coupled atmosphere–ocean models. *J. Hydrol,* **155**, 337–352.

Sellers, P. J., B. W. Meeson, J. Closs, J. Collatz, F. Corprew, D. Dazlich, F. G. Hall, Y. Kerr, R. Koster, S. Los, K. Mitchell, J. McManus, D. Myers, K.-J. Sun, and P. Try. 1995. An overview of the ISLSCP Initiative I—Global data sets. *ISLSCP Initiative I—Global Data Sets for Land–Atmosphere Models, 1987–1988,* NASA, Vols. 1–5, published on CD-ROM (USA_NASA_GDAAC_ISLSCP_001. Overview.doc).

Tarboton, D. G., R. L. Bras, and I. Rodriguez-Iturbe. 1991. The analysis of river basins and channel networks using digital terrain data. *Hydrol. Process,* **5**, 81–100.

Teikoku-Shoin. 1985. *World Atlas (TV-Atlas),* Teikoku-Shoin, Tokyo, 126 pp.

Vörösmarty, C. J., III, A. Grace, B. Peterson, E. Rastetter, and J. Melillo. 1991. Distributed parameter models to analyze the impact of human disturbance of the surface hydrology of a large tropical drainage basin in southern Africa. *Hydrology for the Water Management of Large River Basins,* F. H. M. van de Ven, D. Gutknecht, D. P. Loucks, and K. A. Salewicz, IAHS, IAHS Publ. No. 201, 233–244.

Vörösmarty, C. J., III, B. Moore, M. Gildea, B. Peterson, J. Melillo, D. Kicklighter, J. Raich, E. Rastetter, and P. Steudler. 1989. A continental-scale model of water balance and fluvial transport: Application to South America. *Global Biogeochemical Cycles,* **3**, 241–265.

Vörösmarty, C. J., III, K. Sharma, B. A. H. Fekete, A. H. Copeland, J. Holden, J. Marble, and J. Lough. 1997. The storage and aging of continental runoff in large reservoir systems of the world. *Ambio,* **26**, 210–219.

Wessel, P. and W. H. F. Smith. 1995. New version of the generic mapping tools released. *Eos, Trans. Am. Geophys. Union,* **76**,329.

Table 1. River catalog identified in Total Runoff Integrating Pathways (TRIP). River basins on Antarctica and Greenland in TRIP are excluded and the sequential number in the order of area is not continuous. Representative names of rivers are shown. The river mouth may be shifted within ±1° to the actual location. Basin area and river length in TRIP are compared with previously published numbers. Number of 1° × 1° grid boxes in each river basin is listed at theend of each row.

No.	Name	River mouth		Basin area (10^4 km²)				River length (km)			Grids
		Long	Lat	A_T*	A_O+	A_K#	A_M@	L_T&	L_K**	L_R++	
1	Amazon	50.5°W	0.5°N	614	615	691	615	4434	6280	6300	505
2	Congo	12.5°E	5.5°S	373	369	382	382	3982	4370	4370	305
3	Mississippi	90.5°W	29.5°N	325	325	322	327	4023	5985	6210	347
4	Ob	70.5°E	66.5°N	300	298	299	250	4157	—	5200	441
5	Parana	57.5°W	34.5°S	297	310	297	283	3113	4700	4800	265
6	Nile	30.5°E	31.5°N	296	301	287	296	5464	6670	6690	249
7	Yenisey	83.5°E	71.5°N	261	259	258	258	4757	—	4130	409
8	Lena	124.5°E	73.5°N	235	—	249	250	4292	4400	4270	400
9	Niger	6.5°E	5.5°N	211	209	209	121	3475	4160	4180	177
10	Amur	140.5°E	53.5°N	187	205	185	185	3490	—	4350	234
11	Changjiang	120.5°E	31.5°N	182	181	180	194	4327	5520	6300	171
12	Mackenzie	134.5°W	68.5°N	175	167	180	181	3075	4240	4240	289
13	Volga	48.5°E	46.5°N	141	142	136	—	2973	3350	3690	202
14	Zambeze	36.5°E	18.5°S	133	133	133	120	2419	2660	2740	112
15	Lake Eyre	137.5°E	27.5°S	123	—	124	—	1178	2000	—	111
16	Nelson	92.5°W	57.5°N	111	106	107	—	2285	2600	2570	144
17	St. Lawrence	70.5°W	47.5°N	111	125	129	103	2794	3060	3060	128
18	Murray	139.5°E	35.5°S	107	108	106	106	1883	3490	2590	102
19	Ganges	88.5°E	22.5°N	103	110	95	—	1970	—	2510	93
20	Orange	16.5°E	28.5°S	100	102	102	102	1576	1860	2090	91
21	Indus	67.5°E	24.5°N	97	96	96	97	2518	3180	2900	92
22	Orinoco	61.5°W	9.5°N	95	94	100	99	2000	2740	2060	78
23	Chari	14.5°E	12.5°N	92	88	88	—	1415	1400	1400	76
24	Tocantins	48.5°W	1.5°S	87	90	—	—	2099	—	—	72
25	Yukon	164.5°W	62.5°N	85	90	85	84	2665	3000	3700	158
26	Danube	29.5°E	45.5°N	81	82	82	81	2091	2860	2860	94
27	Mekong	106.5°E	10.5°N	80	80	81	79	3383	4500	4020	69
28	Cubango	22.5°E	19.5°S	79	78	78	—	1112	1800	1800	68
29	Huanghe	118.5°E	37.5°N	78	75	74	77	3823	4670	5460	79
30	Euphrates	48.5°E	30.5°N	76	76	75	105	1986	2760	2800	75
31	Jubba	42.5°E	0.5°N	74	—	75	—	1603	1600	1660	60
32	Columbia	123.5°W	46.5°N	72	65	67	67	1593	1950	1850	84
33	Brahmaputra	90.5°E	22.5°N	65	66	58	—	2769	3000	2900	60
34	Kolyma	160.5°E	69.5°N	64	63	65	64	1947	2130	2600	123
35	Colorado	114.5°W	31.5°N	64	—	63	64	1578	2180	2320	64
36	Rio Grande	97.5°W	26.5°N	61	57	57	—	2044	2880	3030	58
37	Sao Francisco	37.5°W	10.5°S	61	66	60	64	2228	2800	3200	51
38	Dniepr	32.5°E	46.5°N	51	51	50	—	1534	2200	2290	66
39	Amu Darya	59.5°E	43.5°N	49	46	31	—	1987	—	2540	51
40	Limpopo	33.5°E	24.5°S	44	44	44	41	1084	1600	1770	39
41	Senegal	16.5°W	16.5°N	44	44	44	—	1332	1430	1630	37
42	Tarim	86.5°E	41.5°N	44	—	45	—	1379	2000	2180	46
43	Don	39.5°E	47.5°N	43	43	42	—	1238	1870	1970	53
44	Syr Darya	61.5°E	45.5°N	42	65	22	—	1703	2210	2210	46

Table 1. Continued.

No.	Name	River mouth Long	River mouth Lat	A_T*	A_O^+	$A_K^\#$	$A_M^@$	$L_T^\&$	L_K**	L_R^{++}	Grids
45	Xi	113.5°E	22.5°N	41	44	44	44	1115	—	1960	36
47	Volta	0.5°E	6.5°N	38	39	39	—	1129	1600	—	31
49	Northern Dvina	40.5°E	64.5°N	36	36	36	35	1289	—	1750	62
50	Khatanga	106.5°E	73.5°N	36	—	36	—	1092	1636	—	87
52	Irrawaddy	95.5°E	16.5°N	35	43	41	43	1586	2300	2090	31
53	Indigirka	149.5°E	71.5°N	35	36	36	36	1607	1726	—	72
54	Salado	66.5°W	37.5°S	33	—	—	—	1068	—	—	32
55	Godavari	81.5°E	16.5°N	33	31	31	31	1007	1500	—	28
56	Salween	97.5°E	16.5°N	32	—	32	—	2382	2820	2410	29
57	Paranaiba	42.5°W	3.5°S	32	—	32	—	975	1450	—	26
59	Pechora	53.5°E	68.5°N	31	32	32	—	1407	1810	1810	60
62	Salado	57.5°W	35.5°S	29	—	—	—	887	—	—	29
63	Dulce	62.5°W	30.5°S	29	—	—	—	948	—	—	27
65	Magdalena	74.5°W	10.5°N	27	26	24	24	1022	1530	1540	22
66	Churchill	94.5°W	58.5°N	27	—	28	—	1483	1600	—	38
67	Neva	30.5°E	59.5°N	26	28	28	—	711	—	—	42
69	Helmand	62.5°E	30.5°N	24	—	25	—	769	1150	—	23
70	Tugaj	62.5°E	47.5°N	24	—	—	—	630	—	—	30
71	Krishna	80.5°E	16.5°N	24	25	26	—	751	1290	—	20
72	Ural	51.5°E	47.5°N	23	22	24	—	1284	2430	2530	30
73	Fraser	122.5°W	49.5°N	23	22	22	22	911	1110	—	30
74	Yana	135.5°E	71.5°N	23	—	24	22	1002	872	—	47
75	Rhein	4.5°E	51.5°N	23	22	22	—	986	1360	1320	28
76	Huai He	119.5°E	33.5°N	22	—	22	26	663	900	—	21
78	Olenek	120.5°E	72.5°N	20	—	22	—	1560	2270	2160	45
79	Ogooue	9.5°E	1.5°S	20	—	20	—	693	850	—	16
80	Wisla	18.5°E	53.5°N	19	—	20	—	826	1090	1090	25
81	Anadyr	176.5°E	64.5°N	19	—	19	—	811	1150	—	37
82	Liao	122.5°E	40.5°N	19	—	23	17	936	1350	1430	21
83	Rufiji	38.5°E	7.5°S	18	—	18	18	598	1400	—	15
84	Kura	48.5°E	39.5°N	18	—	19	—	819	1360	—	19
86	P'asina	86.5°E	73.5°N	17	—	18	—	972	818	—	43
88	Chao Phraya	100.5°E	13.5°N	16	—	16	—	749	1200	—	14
89	Hai	117.5°E	39.5°N	16	—	14	—	631	—	—	17
91	Taz	78.5°E	67.5°N	16	—	15	—	902	1400	—	31
92	Lake Rudolf	35.5°E	3.5°N	16	—	—	—	801	—	—	13
94	Albany	81.5°W	52.5°N	16	—	13	—	949	975	—	20
95	Koksoak	68.5°W	58.5°N	15	—	13	—	638	1300	—	22
96	Ili	74.5°E	45.5°N	15	—	14	—	1059	1000	1400	17
97	Red	105.5°E	20.5°N	15	—	14	12	666	1200	—	13
98	Essequibo	58.5°W	6.5°N	15	—	15	—	442	970	—	12
99	Cuanza	13.5°E	9.5°S	15	—	15	—	817	630	—	12
100	Telon	100.5°W	64.5°N	14	—	14	—	541	—	—	25
101	Elbe	9.5°E	53.5°N	14	—	15	—	783	1110	1170	18
102	Santiago	104.5°W	21.5°N	14	—	—	—	616	960	—	12
103	Emba	53.5°E	46.5°N	14	—	—	—	478	—	—	16
104	Barito	114.5°E	3.5°S	14	—	—	—	535	—	—	11
105	Fitzroy	150.5°E	23.5°S	13	—	14	—	457	960	—	12
106	Mobile	88.5°W	30.5°N	13	—	11	—	698	1064	—	13

Table 1. Continued.

No.	Name	River mouth		Basin area (10^4 km^2)				River length (km)			Grids
		Long	Lat	A_T*	A_O+	A_K#	A_M@	L_T&	L_K**	L_R++	
107	Sanaga	10.5°E	4.5°N	13	—	13	—	646	860	—	11
108	Ruvuma	39.5°E	11.5°S	13	—	14	—	547	800	—	11
110	Cunene	12.5°E	17.5°S	13	—	14	—	698	830	—	11
111	Usumacinta	92.5°W	18.5°N	13	—	12	—	461	—	—	11
112	Mahanadi	86.5°E	20.5°N	13	—	13	—	720	858	—	11
113	Burdekin	147.5°E	20.5°S	13	—	13	—	373	680	—	11
114	Narmada	72.5°E	21.5°N	13	—	10	—	1071	1300	—	11
116	Brazos	95.5°W	29.5°N	12	—	—	—	1006	1400	—	12
118	Tedzen	61.5°E	36.5°N	12	—	7	—	681	1124	—	12
119	Pur	77.5°E	67.5°N	12	—	11	—	744	—	—	22
120	Loire	1.5°W	47.5°N	12	—	12	—	624	1110	1020	14
121	Kuskokuim	162.5°W	60.5°N	12	—	12	—	811	—	—	20
123	Kerulen	116.5°E	48.5°N	12	—	12	—	911	1264	—	14
124	Chubut	65.5°W	43.5°S	12	—	14	—	653	850	—	13
126	Flinders	140.5°E	17.5°S	12	—	11	—	720	830	—	10
127	Colorado	96.5°W	28.5°N	12	—	10	—	1039	1450	—	11
129	Save	34.5°E	21.5°S	12	—	11	—	581	680	—	10
131	Negro	63.5°W	40.5°S	12	—	13	10	826	1000	—	12
132	Odra	14.5°E	53.5°N	11	—	11	—	577	907	910	15
133	Mattagami	80.5°W	51.5°N	11	—	—	—	465	—	—	14
134	Bandama	4.5°W	5.5°N	11	—	10	—	534	780	—	9
135	Komoe	3.5°W	5.5°N	11	—	—	—	643	—	—	9
137	Hayes	92.5°W	56.5°N	11	—	11	—	385	—	—	15
138	Santa Cruz	68.5°W	50.5°S	10	—	—	—	451	—	—	13
139	Rhone	4.5°E	43.5°N	10	—	10	9	545	810	810	12
141	Anabar	113.5°E	73.5°N	10	—	10	—	764	939	—	25
142	Tes-Chem	92.5°E	50.5°N	10	—	—	—	492	—	—	13
143	Back	96.5°W	67.5°N	10	—	11	—	864	960	—	20
144	Severn	87.5°W	55.5°N	10	—	10	—	582	976	—	14
145	La Grande Riviere	78.5°W	53.5°N	10	—	—	—	531	—	—	14
146	Neman	21.5°E	55.5°N	10	—	10	—	520	937	—	14
147	Taimyra	99.5°E	75.5°N	10	—	12	—	565	754	—	30
148	Broadback	78.5°W	51.5°N	10	—	—	—	614	—	—	13
153	Tana	40.5°E	2.5°S	10	—	9	—	490	720	—	8
158	Saguenay	70.5°W	48.5°N	10	—	9	—	503	—	—	12
159	Gambia	16.5°W	13.5°N	10	—	18	—	590	1200	—	8
170	Balsas	102.5°W	18.5°N	9	—	11	—	422	—	—	8
172	Doce	40.5°W	19.5°S	9	—	8	—	363	600	—	8
174	Douro	8.5°W	41.5°N	9	—	9	—	501	925	—	10
178	Ebro	0.5°E	40.5°N	9	—	9	—	581	930	930	10
186	Panuco	98.5°W	22.5°N	9	—	8	—	318	—	—	8
191	Western Dvina	24.5°E	56.5°N	9	—	9	—	633	1020	—	13
195	Gascoyne	113.5°E	24.5°S	9	—	8	—	553	770	—	8
200	Garonne	0.5°W	44.5°N	9	—	9	—	328	650	—	10
201	Churchill	58.5°W	54.5°N	9	—	8	—	590	560	—	12
224	Tagus Tejo	8.5°W	39.5°N	9	—	8	—	654	1010	—	9
225	Sacramento	121.5°W	38.5°N	9	—	7	—	474	610	—	9
238	Nistru	30.5°E	46.5°N	8	—	7	—	567	—	—	10

Table 1. Continued.

No.	Name	River mouth Long	Lat	Basin area (10^4 km²) A_T*	A_O+	A_K#	A_M@	River length (km) L_T&	L_K**	L_R++	Grids
240	Sarysu	66.5°E	45.5°N	8	—	8	—	700	761	—	10
241	Victoria	129.5°E	15.5°S	8	—	8	—	542	570	—	7
247	Fitzroy	123.5°E	17.5°S	8	—	9	—	412	520	—	7
248	Seine	0.5°E	49.5°N	8	—	8	—	413	780	780	10
257	Mezen	44.5°E	65.5°N	8	—	8	—	584	966	—	15
267	Ashburton	115.5°E	22.5°S	8	—	8	—	505	640	—	7
269	San Joaquin	121.5°W	37.5°N	8	—	8	—	373	560	—	8
281	Rio Colorado	62.5°W	39.5°S	8	—	6	—	772	1000	—	8
284	Guadiana	7.5°W	37.5°N	8	—	7	—	600	800	—	8
285	Penzina	164.5°E	62.5°N	8	—	7	—	509	713	—	14
305	Susquehana	76.5°W	39.5°N	7	—	7	—	361	733	—	8
313	Mamberamo	138.5°E	2.5°S	7	—	8	—	379	—	—	6
316	Sepik	144.5°E	4.5°S	7	—	8	—	333	700	—	6
317	Mearim	44.5°W	3.5°S	7	—	9	—	424	800	—	6
323	Fly	143.5°E	8.5°S	7	—	6	—	644	620	1130	6
324	Sassandra	6.5°W	5.5°N	7	—	7	—	378	660	—	6
331	Nottaway	79.5°W	51.5°N	7	—	6	—	521	—	—	9
342	Mitchell	142.5°E	15.5°S	7	—	7	—	308	520	—	6
356	Nadym	72.5°E	66.5°N	7	—	6	—	662	545	—	13
368	Paraiba	41.5°W	21.5°S	7	—	6	—	461	800	—	6
371	Attawapiskat	82.5°W	52.5°N	7	—	5	—	606	810	—	9
385	Murchison	114.5°E	27.5°S	7	—	7	—	447	700	—	6
392	Yalu	124.5°E	40.5°N	6	—	6	—	530	1500	—	7
415	Apalachicola	84.5°W	30.5°N	6	—	5	—	546	880	—	6
420	Kuban	37.5°E	45.5°N	6	—	6	—	508	870	—	7
421	Kouilou	12.5°E	4.5°S	6	—	6	—	424	600	—	5
426	Po	11.5°E	45.5°N	6	—	7	7	371	650	680	7
435	Lurio	40.5°E	13.5°S	6	—	6	—	478	560	—	5
443	Alazeja	154.5°E	70.5°N	6	—	6	—	513	498	—	13
451	Guadalquivir	6.5°W	37.5°N	6	—	6	—	494	560	—	6
462	Chu	105.5°E	19.5°N	6	—	6	—	257	1190	—	5
471	Kemi	25.5°E	66.5°N	6	—	5	—	312	—	—	12
473	Sakarya	30.5°E	40.5°N	6	—	6	—	539	790	—	6
476	Fortescue	116.5°E	21.5°S	6	—	5	—	255	670	—	5
509	Copper	144.5°W	60.5°N	5	—	6	6	358	360	—	9
514	Onega	38.5°E	63.5°N	5	—	6	—	369	416	—	9
529	Saint John	66.5°W	45.5°N	5	—	6	—	346	640	—	6
533	Skeena	129.5°W	54.5°N	5	—	5	—	385	510	—	7
579	Narva	27.5°E	58.5°N	5	—	6	—	299	77	—	7

*River basin area in TRIP.
+River basin area from MO92.
#River basin area from KU78.
@River basin area from MM83.
&River length in TRIP.
**River length from KU78.
++River length by JNAO93.

Table 2a. Number of grid boxes with river channel of each direction, before and after the manual corrections for the first guess by the lowest neighbor algorithm. There are 1162 grid boxes pointing southwest (SW) after the manual correction (column 8, row 13), but 933 out of 1162 were SW as well before the manual correction (row 8). The grid boxes where the automatic algorithm could not determine the directions are presented as "N/A" (row 12), and for example, 78 of these grid boxes are pointing north (column 3) after the manual correction. The statistic of the correction shows the usefulness of the automated method. Similar statistics for the steepest slope algorithm (Table 2b) showed that lowest neighbor method was equally satisfactory.

Before	Sea	North	NE	East	SE	South	SW	West	NW	Mouth	Total	Changed
Sea	43,082	11	5	13	7	9	6	8	2	1	43,144	62
North	0	3597	54	97	20	17	17	82	29	166	4079	482
NE	0	210	2580	490	57	63	18	130	61	257	3866	1286
East	0	29	27	749	39	33	15	60	16	284	1252	503
SE	0	73	56	369	1090	221	51	118	29	230	2237	1147
South	0	35	16	67	52	548	29	76	20	223	1066	518
SW	0	59	27	103	48	198	933	353	53	223	1997	1064
West	0	46	18	55	11	30	21	749	28	256	1214	465
NW	0	242	56	116	24	53	48	353	2507	228	3627	1120
Mouth	0	8	7	24	4	15	3	21	4	1567	1653	86
N/A	0	78	52	139	55	65	21	94	36	125	665	665
Total	43,082	4388	2898	2222	1407	1252	1162	2044	2785	3560	64,800	
Changed	0	791	318	1473	317	704	229	1295	278	1993	7398	
(%)	0	18	11	66	23	56	20	63	10	56	11	

Table 2b. Same as Table 2a but for the first guess by the steepest slope algorithm.

Before	Sea	North	NE	East	SE	South	SW	West	NW	Mouth	Total	Changed
Sea	43,082	11	5	13	7	9	6	8	2	1	43,144	62
North	0	3692	920	144	38	27	38	134	861	759	6613	2921
NE	0	113	1354	224	35	32	11	73	36	229	2107	753
East	0	141	383	1192	404	143	70	115	91	472	3011	1819
SE	0	38	30	173	522	124	34	60	21	165	1167	645
South	0	50	27	112	254	629	166	102	40	264	1644	1015
SW	0	35	16	58	27	97	440	178	32	153	1036	596
West	0	146	98	118	72	112	349	1124	356	398	2773	1649
NW	0	118	28	73	18	28	33	170	1317	216	2001	684
Mouth	0	2	6	14	1	8	1	10	1	821	864	43
N/A	0	42	31	101	29	43	14	70	28	82	440	440
Total	43,082	4388	2898	2222	1407	1252	1162	2044	2785	3560	64.800	
Changed	0	696	1544	1030	885	623	722	920	1468	2739	10,627	
(%)	0	16	53	46	63	50	62	45	53	77	16	